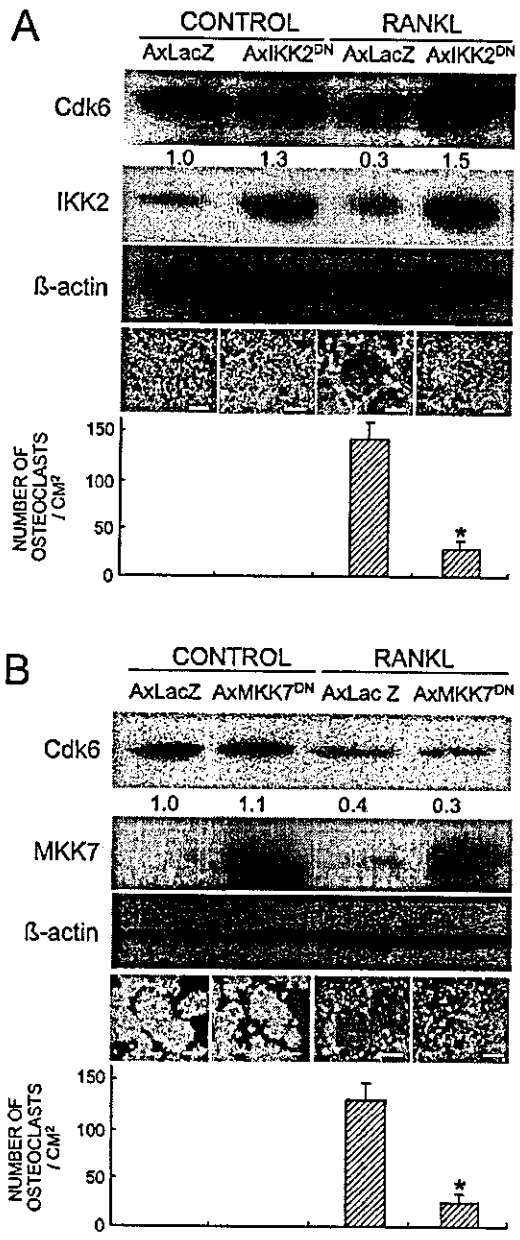

FIG. 2. Effects of overexpression of (A) IKK^{DN} and (B) $MKK7^{DN}$ using adenovirus vectors on the Cdk6 inhibition and osteoclastogenesis by RANKL in the RAW cell culture. RAW cells were infected with a recombinant adenovirus carrying the IKK^{DN}, $MKK7^{DN}$, or *LacZ* gene at 100 MOI, and subsequently, growth-arrested by incubation in a low serum medium for 2 days. The cells were stimulated with serum in the presence or absence of RANKL (100 ng/ml) for 5 days. Bar, 100 μm. Expressions of Cdk6, IKK2, and MKK7 were determined by Western blotting with β-actin as loading controls. The number under each band is the treated/control ratio of the intensity of the Cdk6 band normalized to that of β-actin measured by densitometry. Similar results were obtained in independent Western blottings of three separate experiments. The graph indicates means (bars) $\pm$ SE (error bars) for 8 wells/group. *Significant difference from the RANKL-treated and AxLacZ-infected culture; $p < 0.01$.

Cdk6 cDNA and tested their ability to respond to RANKL and differentiate to osteoclasts. The ability of RANKL to induce $TRACP^+$ multinucleated osteoclast formation was compared among the empty vector-transfected cells and low- (~1.5-fold) and high- (>5-fold) expressing cells. RANKL induced osteoclastogenesis in the empty vector-transfected cells and low-expressing clones; however, it was markedly decreased in high-expressing clones (Fig. 3A). Cdk6-led resistance to osteoclast differentiation is unlikely to be caused by an unexpected interference of the RANKL/NF-κB signaling by the overexpressed Cdk6, because RANK expression was not significantly affected by Cdk6 expression (Fig. 3B).

Overexpression of Cdk6 does not influence cell cycle regulation of osteoclasts

Because Cdk6 promotes the G1-S transition, suppression of osteoclast differentiation by overexpressed Cdk6 could be a mere consequence of its execution of this role. We therefore examined the effects of both RANKL and Cdk6 overexpression on G1-S transition and proliferation of RAW cells. The three kinds of transfected cells were similarly arrested in quiescence, stimulated with serum in the presence and absence of RANKL, and analyzed for cell proliferation and populations in G0/G1 and G2/M by BrdU incorporation and flow cytometric analysis (FACS; Table 1). At 3 days of culture, when osteoclastogenesis just started, RANKL slightly reduced cell proliferation and the G2/M population; however, Cdk6 overexpression caused no significant changes in either of them. These results indicate that the inhibitory effect of Cdk6 on osteoclast differentiation was not exerted through cell cycle regulation.

DISCUSSION

This study showed that Cdk6 is a key molecule in determining the differentiation rate of osteoclasts as a downstream effector of RANKL/NF-κB signaling. Figure 4 shows the mechanism of effect of RANKL on osteoclast differentiation based on present and previous studies. The RANK activation by binding of RANKL stimulates the NF-κB signaling, probably through association with TRAFs.[6,8–11] NF-κB moves from the cytoplasm into the nucleus, associates with various transcription factors in the nucleus, and downregulates Cdk6, which is a negative regulator of the transition from the G1 to the differentiation stage.

This study failed to show the contribution of JNK, another major pathway lying downstream of RANKL, to the RANKL-led Cdk6 downregulation. Our results, however, do not rule out the possibility that pathways other than NF-κB–mediated Cdk6 inhibition are required for osteoclast differentiation. JNK is known to activate activator protein 1 (AP-1), which is composed of various combinations of Fos and Jun family members. Mice deficient in c-*Fos* are reported to be osteopetrotic because of the failure in osteoclast differentiation, which can be rescued by Fra-1 as well as c-*Fos* overexpression,[28–31] indicating a crucial role of the JNK/AP-1 signaling in osteoclastogenesis.[12,13] JNK is activated by the phosphorylation of Thr and Tyr residues through MKK4 and/or MKK7. MKK7 seems to be

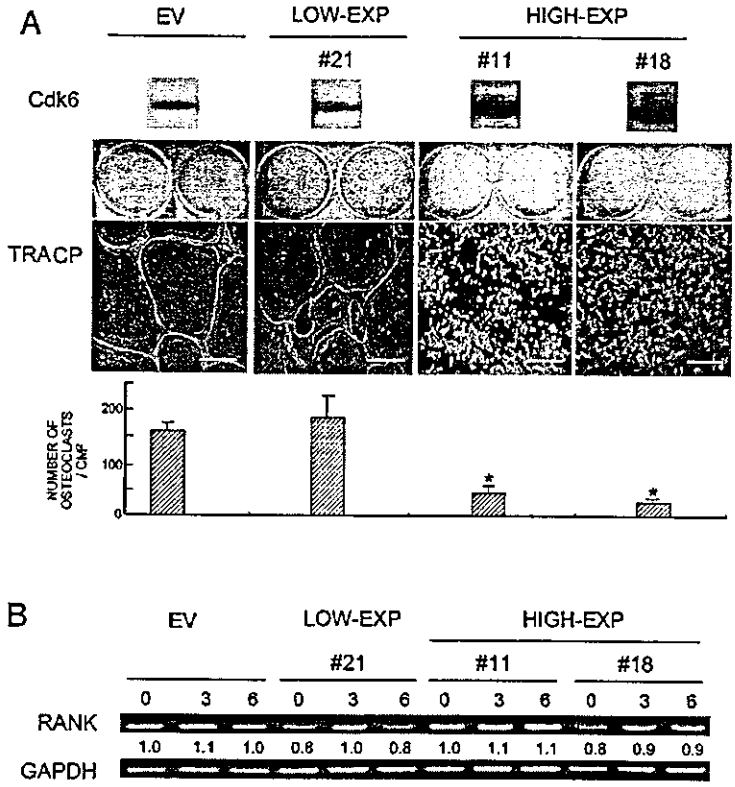

FIG. 3. (A) RANKL-induced osteoclastogenesis from RAW cells overexpressing Cdk6. Stable clones of RAW cells transfected with *Cdk6* cDNA were established as described in the Materials and Methods section, and clones with low expression (21) and high expression (11 and 18) were selected on Western blotting (top panel). These clones and empty vector-transfected RAW (EV) cells were induced for osteoclast differentiation by treating with RANKL (100 ng/ml) for 7 days, and osteoclast formation was determined by TRACP staining. The macroscopic images of culture wells and the microscopic images inside the wells are shown in the middle panels. Bar, 100 μm. The graph in the bottom panel is expressed as means (bars) ± SE (error bars) for 8 wells/group. *Significant difference from the EV cell culture; $p < 0.01$. (B) RANK mRNA levels by RT-PCR in each clone stimulated for 3 and 6 days with RANKL. The number under each band is the intensity of the RANK band normalized to that of GAPDH measured by densitometry. Other clones with low and high expressions showed similar results.

TABLE 1. CELL CYCLE REGULATION OF RAW CELLS OVEREXPRESSING Cdk6

	BrdU (OD)		*FACS*			
			G0/G1 (%)		*G2/M (%)*	
	RANKL⁻	*RANKL⁺*	*RANKL⁻*	*RANKL⁺*	*RANKL⁻*	*RANKL⁺*
EV	0.52 ± 0.03	0.39 ± 0.03*	75.2 ± 0.5	78.7 ± 0.7	15.9 ± 0.6	12.3 ± 0.6†
#21 (Low)	0.52 ± 0.05	0.34 ± 0.04*	75.5 ± 0.2	78.0 ± 0.4	16.1 ± 0.5	12.6 ± 0.5†
#11 (High)	0.56 ± 0.10	0.45 ± 0.03†	74.8 ± 0.9	78.9 ± 0.7	16.3 ± 0.9	12.2 ± 0.8†
#18 (High)	0.56 ± 0.08	0.39 ± 0.06†	75.7 ± 0.6	77.9 ± 0.9	16.7 ± 1.1	11.9 ± 0.6†

Cell proliferation was determined by BrdU incorporation into EV, low-expressing and high-expressing clones in the presence and absence of RANKL at 3 days of culture. Cell cycle distribution of mononuclear cells was determined by FACS, and percentages of cells in each cell cycle stage (G0/G1 and G2/M) are shown. Data are expressed as the mean ± SD for 6 wells/clone. Cdk6 overexpression did not significantly affect the cell proliferation and the cell cycle distribution. RANKL treatment reduced the cell proliferation and the cell population at G2/M.

*$p < 0.001$; †$p < 0.01$ significant inhibition by RANKL.

more specific in JNK activation than MKK4 because MKK4 is known to activate p38 MAPK as well. We previously reported that overexpression of $MKK7^{DN}$ in RAW cells by the adenovirus vector inhibited both RANKL-induced JNK activation and osteoclast formation.[21] JNK may possibly contribute to osteoclast differentiation through an independent pathway of Cdk6. Other possible pathways for osteoclast differentiation are the p38 MAPK and the Smad signaling. Recently, Matsumoto et al.[32] reported that RANKL activates p38 pathways in osteoclast precursors, which is essential for osteoclast differentiation, and Fuller et al.[33] and Kaneda et al.[34] showed the critical role of transforming growth factor (TGF)-β in osteoclast differentiation and survival. The involvement of cell cycle factors in osteoclast differentiation mediated by these pathways should be clarified in the future.

Cdk6 overexpression did not affect cell cycle regulation of RAW cells. D cyclins and partner kinases Cdk4 and Cdk6 are all known to be critical factors that control the cell growth potential,[35,36] but several specific roles have been reported for Cdk6. The Cdk6-cyclin D3 complex is unique among cyclin D and cognate kinase combinations and

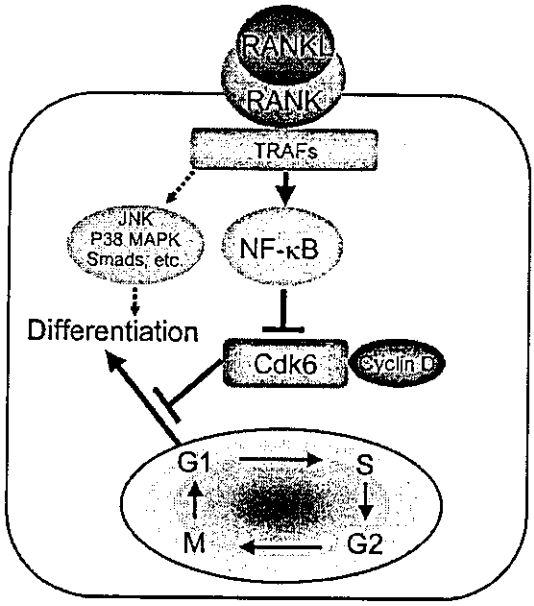

FIG. 4. Scheme of Cdk6-dependent RANKL effect on osteoclast differentiation obtained from this study. RANKL stimulates NF-κB signaling by binding to RANK through association with TRAFs. NF-κB downregulates Cdk6, which is a negative regulator of the transition from the G1 phase to the differentiation stage. Other signaling pathways such as JNK, p38 MAPK, and Smads might be involved in osteoclast differentiation through mechanisms independent of Cdk6.

evades inhibition by CKIs.[25] Therefore, it can greatly enhance the proliferative potential of fibroblasts under growth-suppressive conditions,[25] and consequently, sensitizes cells to physical and chemical transformation.[37] Cdk6 combined with cyclin K, encoded by human herpes virus 8, which is the causative agent of Kaposi sarcoma, is also reported to be immune to inhibition by CKIs.[38] These functions were not seen in Cdk4 complexes. This study discovered a novel function of Cdk6 as an inhibitor of the transition to the differentiation stage without affecting cell cycle regulation. Although Cdk4 has 70% homology of amino acid sequence with Cdk6,[27] the Cdk4 protein was not affected by RANKL in this study. We hereby propose that Cdk4 and Cdk6 play different roles and that Cdk4 cannot substitute for Cdk6 in osteoclastic cells.

How could Cdk6 control differentiation without influencing cell cycling? One possibility is that Cdk6 directly controls a factor critically involved in differentiation. This possibility may not be as remote as generally thought. In fission yeast, Pas1 cyclin and its partner kinase Pef1 activate a transcription factor complex functionally equivalent to E2F-DP of mammals, thereby promoting S phase entry, just like Cdk6, yet they independently inhibit the mating pheromone signaling whose activation is essential for differentiation of this yeast cell.[39] Thus, this might be a good model for the situation of Cdk6 in RANKL-induced osteoclast differentiation, highlighting a potential functional similarity between Cdk6 and Pef1.

Among cell cycle factors, Cdk's have vital roles in controlling cell cycle progression. Therefore, much attention has been devoted to the view that CKI-led inhibition of G1-specific Cdk's is critical for cell differentiation. Accordingly, potential roles for CKIs in differentiation have been studied extensively, but with mixed results.[40,41] Several studies revealed a certain correlation between induction of $p21^{CIP1}$ and differentiation in hematopoietic cells including monocytes/macrophages.[42-46] For osteoclast differentiation as well, upregulation of $p21^{CIP1}$ and $P27^{KIP1}$ is reported to be associated with osteoclast differentiation in the M-BMMϕ culture.[47] This was inconsistent with the present results in RAW cells that $P27^{KIP1}$ was not increased, but rather decreased, by RANKL and that $p21^{CIP1}$ could not be detected. Mice completely ablated for $p21^{CIP1}$ and/or $P27^{KIP1}$ or other major CKIs still develop and grow normally without significant bone abnormality such as osteopetrosis, strongly dismissing the current view.[41,48] Although there is evidence for $p57^{KIP2}$ being involved in differentiation of some cells,[49,50] no one has identified cell cycle factors that are controlled by differentiation signals and critically influence the differentiation commitment process. Because the Cdk6 downregulation was reproducible in RAW cell and M-BMMϕ cultures, we believe that Cdk6 generally plays a role in the RANKL-induced osteoclast differentiation. Although we tried to perform the signaling and overexpression experiments in M-BMMϕ, adenovirus infection and plasmid transfection were much less efficient in transducing these cells. Matsuo et al.[31] reported an efficient gene transfer into osteoclast precursors using a retrovirus vector system. However, the level of gene expression by retrovirus vectors is not enough for experiments using dominant negative molecules like this study. Developing more efficient gene transduction systems to primary osteoclast precursors will be helpful for further analysis of the signaling pathways of osteoclast differentiation.

This study for the first time showed that Cdk6, a G1 cell cycle factor, plays a critical role in controlling RANKL-induced osteoclast differentiation. Numerous signaling molecules, including transcription factors such as a nuclear factor of activated T-cells (NFATs),[51,52] have recently been reported to be involved in osteoclast differentiation. Consequently, one of these factors may be responsible for the RANKL-triggered repression of Cdk6 transcription. Identification of the transcriptional repressor as well as key targets for Cdk6 will definitely be required for deeper understanding of the molecular basis of bone resorption.

ACKNOWLEDGMENTS

We thank Reiko Yamaguchi for providing expert technical assistance and Drs Inder Verma and Izumu Saito for kindly providing adenovirus vectors carrying $IKK2^{DN}$ and LacZ, respectively. This study was funded by a Grant-in-Aid for Scientific Research from the Japanese Ministry of Education, Science, Sports, Culture and Technology (14657358).

REFERENCES

1. Suda T, Takahashi N, Udagawa N, Jimi E, Gillespie MT, Martin TJ 1999 Modulation of osteoclast differentiation and function by the new members of the tumor necrosis factor receptor and ligand families. Endocr Rev 20:345–357.
2. Lacey DL, Timms E, Tan HL, Kelley MJ, Dunstan CR, Burgess T, Elliott R, Colombero A, Elliott G, Scully S, Hsu H, Sullivan J, Hawkins N, Davy E, Capparelli C, Eli A, Qian YX, Kaufman S, Sarosi I, Shalhoub V, Senaldi G, Guo J, Delaney J, Boyle WJ 1998 Osteoprotegerin ligand is a cytokine that regulates osteoclast differentiation and activation. Cell 93:165–176.
3. Yasuda H, Shima N, Nakagawa N, Yamaguchi K, Kinosaki M, Mochizuki S, Tomoyasu A, Yano K, Goto M, Murakami A, Tsuda E, Morinaga T, Higashio K, Udagawa N, Takahashi N, Suda T 1998 Osteoclast differentiation factor is a ligand for osteoprotegerin/osteoclastogenesis-inhibitory factor and is identical to TRANCE/RANKL. Proc Natl Acad Sci USA 95:3597–3602.
4. Kong YY, Boyle WJ, Penninger JM 1999 Osteoprotegerin ligand: A common link between osteoclastogenesis, lymph node formation and lymphocyte development. Immunol Cell Biol 77:188–193.
5. Kong YY, Yoshida H, Sarosi I, Tan HL, Timms E, Capparelli C, Morony S, Oliveira-dos-Santos AJ, Van G, Itie A, Khoo W, Wakeham A, Dunstan CR, Lacey DL, Mak TW, Boyle WJ, Penninger JM 1999 OPGL is a key regulator of osteoclastogenesis, lymphocyte development and lymph-node organogenesis. Nature 397:315–323.
6. Li J, Sarosi I, Yan XQ, Morony S, Capparelli C, Tan HL, McCabe S, Elliott R, Scully S, Van G, Kaufman S, Juan SC, Sun Y, Tarpley J, Martin L, Christensen K, McCabe J, Kostenuik P, Hsu H, Fletcher F, Dunstan CR, Lacey DL, Boyle WJ 2000 RANK is the intrinsic hematopoietic cell surface receptor that controls osteoclastogenesis and regulation of bone mass and calcium metabolism. Proc Natl Acad Sci USA 97:1566–1571.
7. Nakagawa N, Kinosaki M, Yamaguchi K, Shima N, Yasuda H, Yano K, Morinaga T, Higashio K 1998 RANK is the essential signaling receptor for osteoclast differentiation factor in osteoclastogenesis. Biochem Biophys Res Commun 253:395–400.
8. Darnay BG, Haridas V, Ni J, Moore PA, Aggarwal BB 1998 Characterization of the intracellular domain of receptor activator of NF-κB (RANK). Interaction with tumor necrosis factor receptor-associated factors and activation of NF-κB and c-Jun N-terminal kinase. J Biol Chem 273:20551–20555.
9. Darnay BG, Ni J, Moore PA, Aggarwal BB 1999 Activation of NF-κB by RANK requires tumor necrosis factor receptor-associated factor (TRAF) 6 and NF-kappaB-inducing kinase. Identification of a novel TRAF6 interaction motif. J Biol Chem 274:7724–7731.
10. Galibert L, Tometsko ME, Anderson DM, Cosman D, Dougall WC 1998 The involvement of multiple tumor necrosis factor receptor (TNFR)-associated factors in the signaling mechanisms of receptor activator of NF-kappaB, a member of the TNFR superfamily. J Biol Chem 273:34120–34127.
11. Lomaga MA, Yeh WC, Sarosi I, Duncan GS, Furlonger C, Ho A, Morony S, Capparelli C, Van G, Kaufman S, van der Heiden A, Itie A, Wakeham A, Khoo W, Sasaki T, Cao Z, Penninger JM, Paige CJ, Lacey DL, Dunstan CR, Boyle WJ, Goeddel DV, Mak TW 1999 TRAF6 deficiency results in osteopetrosis and defective interleukin-1, CD40, and LPS signaling. Genes Dev 13:1015–1024.
12. Iotsova V, Caamano J, Loy J, Yang Y, Lewin A, Bravo R 1997 Osteopetrosis in mice lacking NF-kappaB1 and NF-kappaB2. Nat Med 3:1285–1289.
13. Franzoso G, Carlson L, Xing L, Poljak L, Shores EW, Brown KD, Leonardi A, Tran T, Boyce BF, Siebenlist U 1997 Requirement for NF-kappaB in osteoclast and B-cell development. Genes Dev 11:3482–3496.
14. Verma IM, Stevenson J 1997 IkappaB kinase: Beginning, not the end. Proc Natl Acad Sci USA 94:11758–11760.
15. Karin M 1999 The beginning of the end: IkappaB kinase (IKK) and NF-kappaB activation. J Biol Chem 274:27339–27342.
16. Ghosh S 1999 Regulation of inducible gene expression by the transcription factor NF-kappaB. Immunol Res 19:183–189.
17. Li Q, Van Antwerp D, Mercurio F, Lee KF, Verma IM 1999 Severe liver degeneration in mice lacking the IkappaB kinase 2 gene. Science 284:321–325.
18. Li Q, Lu Q, Hwang JY, Buscher D, Lee KF, Izpisua-Belmonte JC, Verma IM 1999 IKK1-deficient mice exhibit abnormal development of skin and skeleton. Genes Dev 13:1322–1328.
19. Li ZW, Chu W, Hu Y, Delhase M, Deerinck T, Ellisman M, Johnson R, Karin M 1999 The IKKbeta subunit of IkappaB kinase (IKK) is essential for nuclear factor kappaB activation and prevention of apoptosis. J Exp Med 189:1839–1845.
20. Rudolph D, Yeh WC, Wakeham A, Rudolph B, Nallainathan D, Potter J, Elia AJ, Mak TW 2000 Severe liver degeneration and lack of NF-kappaB activation in NEMO/IKKgamma-deficient mice. Genes Dev 14:854–862.
21. Yamamoto A, Miyazaki T, Kadono Y, Takayanagi H, Miura T, Nishina H, Katada T, Wakabayashi K, Oda H, Nakamura K, Tanaka S 2002 Possible involvement of IkappaB kinase 2 and MKK7 in osteoclastogenesis induced by receptor activator of nuclear factor kappaB ligand. J Bone Miner Res 17:612–621.
22. Sherr CJ 1994 G1 phase progression: Cycling on cue. Cell 79:551–555.
23. Sherr CJ, Roberts JM 1999 CDK inhibitors: Positive and negative regulators of G1-phase progression. Genes Dev 13:1501–1512.
24. Vidal A, Koff A 2000 Cell-cycle inhibitors: Three families united by a common cause. Gene 247:1–15.
25. Kobayashi K, Takahashi N, Jimi E, Udagawa N, Takami M, Kotake S, Nakagawa N, Kinosaki M, Yamaguchi K, Shima N, Yasuda H, Morinaga T, Higashio K, Martin TJ, Suda T 2000 Tumor necrosis factor alpha stimulates osteoclast differentiation by a mechanism independent of the ODF/RANKL-RANK interaction. J Exp Med 191:275–286.
26. Lin J, Jinno S, Okayama H 2001 Cdk6-cyclin D3 complex evades inhibition by inhibitor proteins and uniquely controls cell's proliferation competence. Oncogene 20:2000–2009.
27. Meyerson M, Enders GH, Wu CL, Su LK, Gorka C, Nelson C, Harlow E, Tsai LH 1992 A family of human cdc2-related protein kinases. EMBO J 11:2909–2917.
28. Wang ZQ, Ovitt C, Grigoriadis AE, Mohle-Steinlein U, Ruther U, Wagner EF 1992 Bone and haematopoietic defects in mice lacking *c-fos*. Nature 360:741–745.
29. Johnson RS, Spiegelman BM, Papaioannou V 1992 Pleiotropic effects of a null mutation in the c-fos proto-oncogene. Cell 71:577–586.
30. Grigoriadis AE, Wang ZQ, Cecchini MG, Hofstetter W, Felix R, Fleisch HA, Wagner EF 1994 c-Fos: A key regulator of osteoclast-macrophage lineage determination and bone remodeling. Science 266:443–448.
31. Matsuo K, Owens JM, Tonko M, Elliott C, Chambers TJ, Wagner EF 2000 Fosl1 is a transcriptional target of c-Fos during osteoclast differentiation. Nat Genet 24:184–187.
32. Matsumoto M, Sudo T, Saito T, Osada H, Tsujimoto M 2000 Involvement of p38 mitogen-activated protein kinase signaling pathway in osteoclastogenesis mediated by receptor activator of NF-kappa B ligand (RANKL). J Biol Chem 275:31155–31161.
33. Fuller K, Lean JM, Bayley KE, Wani MR, Chambers TJ 2000 A role for TGFbeta(1) in osteoclast differentiation and survival. J Cell Sci 113:2445–2453.
34. Kaneda T, Nojima T, Nakagawa M, Ogasawara A, Kaneko H, Sato T, Mano H, Kumegawa M, Hakeda Y 2000 Endogenous production of TGF-beta is essential for osteoclastogenesis induced by a combination of receptor activator of NF-kappaB ligand and macrophage-colony-stimulating factor. J Immunol 165:4254–4263.
35. Baldin V, Lucus J, Marcote MJ, Pagano M, Draetta G 1993 Cyclin D1 is a nuclear protein required for cell cycle progression in G_1. Genes Dev 7:812–821.
36. Hengstchlager M, Braun K, Soucek A, Miloloza E, Hengstchlager O 1999 Cyclin-dependent kinases at the G_1-S transition of the mammalian cell cycle. Mutat Res 436:1–9.
37. Chen Q, Lin J, Jinno S, Okayama H 2003 Overexpression of Cdk6-cyclin D3 highly sensitizes cells to physical and chemical transformation. Oncogene 22:992–1001.
38. Swanton C, Mann DJ, Fleckenstein B, Neipel F, Peters G, Jones N 1997 Herpes viral cyclin/Cdk6 complexes evade inhibition by CDK inhibitor proteins. Nature 390:184–187.
39. Tanaka K, Okayama H 2000 A pcl-like cyclin activates the Res2p-Cdc10p cell cycle "start" transcriptional factor complex in fission yeast. Mol Biol Cell 11:2845–2862.
40. Missero C, Di Cunto F, Kiyokawa H, Koff A, Dotto GP 1996 The absence of p21Cip1/WAF1 alters keratinocyte growth and differ-

entiation and promotes ras-tumor progression. Genes Dev 10: 3065–3075.
41. Deng C, Zhang P, Harper JW, Elledge SJ, Leder P 1995 Mice lacking p21CIP1/WAF1 undergo normal development, but are defective in G1 checkpoint control. Cell 82:675–684.
42. Steinman RA, Hoffman B, Iro A, Guillouf C, Liebermann DA, el-Houseini ME 1994 Induction of p21 (WAF-1/CIP1) during differentiation. Oncogene 9:3389–3396.
43. Schwaller J, Koeffler HP, Niklaus G, Loetscher P, Nagel S, Fey MF, Tobler A 1995 Posttranscriptional stabilization underlies p53-independent induction of p21WAF1/CIP1/SDI1 in differentiating human leukemic cells. J Clin Invest 95:973–979.
44. Freemerman AJ, Vrana JA, Tombes RM, Jiang H, Chellappan SP, Fisher PB, Grant S 1997 Effects of antisense p21 (WAF1/CIP1/MDA6) expression on the induction of differentiation and drug-mediated apoptosis in human myeloid leukemia cells (HL-60). Leukemia 11:504–513.
45. Liu M, Lee MH, Cohen M, Bommakanti M, Freedman LP 1996 Transcriptional activation of the Cdk inhibitor p21 by vitamin D3 leads to the induced differentiation of the myelomonocytic cell line U937. Genes Dev 10:142–153.
46. Muto A, Kizaki M, Yamato K, Kawai Y, Kamata-Matsushita M, Ueno H, Ohguchi M, Nishihara T, Koeffler HP, Ikeda Y 1999 1,25-dihydroxyvitamin D3 induces differentiation of a retinoic acid-resistant acute promyelocytic leukemia cell line (UF-1) associated with expression of p21(WAF1/CIP1) and p27(KIP1). Blood 93:2225–2233.
47. Okahashi N, Murase Y, Koseki T, Sato T, Yamato K, Nishihara T 2001 Osteoclast differentiation is associated with transient upregulation of cyclin-dependent kinase inhibitors p21(WAF1/CIP1) and p27(KIP1). J Cell Biochem 80:339–345.
48. Nakayama K, Ishida N, Shirane M, Inomata A, Inoue T, Shishido N, Horii I, Loh DY 1996 Mice lacking p27(Kip1) display increased body size, multiple organ hyperplasia, retinal dysplasia, and pituitary tumors. Cell 85:707–720.
49. Yan Y, Frisen J, Lee MH, Massague J, Barbacid M 1997 Ablation of the CDK inhibitor p57Kip2 results in increased apoptosis and delayed differentiation during mouse development. Genes Dev 11:973–983.
50. Zhang P, Liegeois NJ, Wong C, Finegold M, Hou H, Thompson JC, Silverman A, Harper JW, DePinho RA, Elledge SJ 1997 Altered cell differentiation and proliferation in mice lacking p57KIP2 indicates a role in Beckwith-Wiedemann syndrome. Nature 387:151–158.
51. Takayanagi H, Kim S, Koga T, Nishina H, Isshiki M, Yoshida H, Saiura A, Isobe M, Yokochi T, Inoue J, Wagner EF, Mak TW, Kodama T, Taniguchi T 2002 Induction and activation of the transcription factor NFATc1 (NFAT2) integrate RANKL signaling in terminal differentiation of osteoclasts. Dev Cell 3:889–901.
52. Ishida N, Hayashi K, Hoshijima M, Ogawa T, Koga S, Miyatake Y, Kumegawa M, Kimura T, Takeya T 2002 Large scale gene expression analysis of osteoclastogenesis in vitro and elucidation of NFAT2 as a key regulator. J Biol Chem 277:41147–41156.

Address reprint requests to:
Hiroshi Kawaguchi, MD, PhD
Department of Orthopaedic Surgery
Faculty of Medicine
University of Tokyo
Hongo 7-3-1, Bunkyo
Tokyo 113-8655, Japan
E-mail: kawaguchi-ort@h.u-tokyo.ac.jp

Received in original form August 10, 2003; in revised form February 5, 2004; accepted March 11, 2004.

MOLECULAR AND CELLULAR BIOLOGY, Aug. 2004, p. 6560–6568
0270-7306/04/$08.00+0 DOI: 10.1128/MCB.24.15.6560–6568.2004

Vol. 24, No. 15

Bone Morphogenetic Protein 2-Induced Osteoblast Differentiation Requires Smad-Mediated Down-Regulation of Cdk6

Toru Ogasawara,[1,2] Hiroshi Kawaguchi,[2] Shigeki Jinno,[1] Kazuto Hoshi,[2] Keiji Itaka,[2] Tsuyoshi Takato,[2] Kozo Nakamura,[2] and Hiroto Okayama[1]*

Departments of Biochemistry and Molecular Biology[1] and Sensory and Motor System Medicine,[2] The University of Tokyo Graduate School of Medicine, Tokyo 113-0033, Japan

Received 31 March 2004/Accepted 8 May 2004

Because a temporal arrest in the G_1 phase of the cell cycle is thought to be a prerequisite for cell differentiation, we investigated cell cycle factors that critically influence the differentiation of mouse osteoblastic MC3T3-E1 cells induced by bone morphogenetic protein 2 (BMP-2), a potent inducer of osteoblast differentiation. Of the G_1 cell cycle factors examined, the expression of cyclin-dependent kinase 6 (Cdk6) was found to be strongly down-regulated by BMP-2/Smads signaling, mainly via transcriptional repression. The enforced expression of Cdk6 blocked BMP-2-induced osteoblast differentiation to various degrees, depending on the level of its overexpression. However, neither BMP-2 treatment nor Cdk6 overexpression significantly affected cell proliferation, suggesting that the inhibitory effect of Cdk6 on cell differentiation was exerted by a mechanism that is largely independent of its cell cycle regulation. These results indicate that Cdk6 is a critical regulator of BMP-2-induced osteoblast differentiation and that its Smads-mediated down-regulation is essential for efficient osteoblast differentiation.

Bone morphogenetic protein 2 (BMP-2) is a potent inducer of bone formation through its stimulation of osteoblast differentiation (17). It exerts this effect via two types of serine/threonine kinase receptors: BMP-2 binds the type II receptor, which subsequently activates the type I receptor by a direct association. Signals from the activated type I receptor are transmitted to the nucleus through various mediator molecules, the most important among them being a family of proteins termed Smads. Smads are classified into three subgroups, i.e., Smad1, Smad5, and Smad8 are classified as receptor-regulated Smads (R-Smads), Smad4 is classified as a common-partner Smad (Co-Smad), and Smad6 and Smad7 are classified as inhibitory Smads (I-Smads) (6). R-Smads are directly activated by the type I receptor, form complexes with Co-Smad, and are translocated into the nucleus, where they regulate the transcription of target genes. I-Smads inhibit the activation of R-Smads by interfering with their association with the type I receptor, which results in the hindrance of the assembly of R-Smads with Co-Smad. Although the downstream signaling of the BMP-2/Smad pathway leading to osteoblast differentiation has been extensively investigated, most of the studies have focused on the bone-related transcriptional regulators Runx2/Cbfa1 (7, 31), osterix (12), SIP1 (25), Smurf1 (32), NF-κB (4, 9), Hoxc-8 (1, 20), and Tob (29).

The proliferation of eukaryotic cells depends on their progression through the cell cycle, and an at least temporal cell cycle arrest in the G_1 phase is thought to be a prerequisite for cell differentiation (18). Cell cycle progression is controlled by the action of cyclins and cyclin-dependent protein kinases (Cdks), which phosphorylate and thereby activate cell cycle factors that are essential for the onset of the next cell cycle phase. In mammalian cells, traverse through G_1 and subsequent S-phase entry require the activities of the cyclin D-dependent kinase Cdk4 and/or Cdk6 (11) and the cyclin E-dependent kinase Cdk2. A key physiological substrate for Cdk4 and Cdk6 is the retinoblastoma (Rb) protein, which binds and inactivates the E2F-DP transcription complexes that are essential for S-phase entry. Phosphorylation by Cdk4/6 and additionally by Cdk2 inactivates Rb, thereby releasing E2F-DP from inactivation and consequently promoting S-phase entry and progression (5, 14). These Cdks are negatively regulated by cyclin-dependent kinase inhibitors (CKIs) via direct binding to themselves (19, 26). CKIs have been classified into two families, the INK4 family and the Cip/Kip family. INK4 family members (p16, p15, p18, and p19) inhibit only Cdk4 and Cdk6, whereas Cip/Kip family members (p21, p27, and p57) inhibit all of the Cdks except for the Cdk6-cyclin D3 complex. Because of its unique ability to evade inhibition by Cip/Kip proteins, Cdk6-D3 can control the cell's proliferative potential under growth-suppressive conditions despite its relative minority in level of expression in mesenchymal cells (8).

Cdks play crucial roles in controlling cell cycle progression. Therefore, much attention has been attracted by the view that the CKI-led inhibition of G_1-specific Cdks is critical for cell differentiation. Accordingly, potential roles for CKIs in differentiation have been extensively studied, but with mixed results. Many studies revealed a certain correlation between the induction of $p21^{CIP1}$ and differentiation, yet many did not. Mice with a complete deletion of $p21^{CIP1}$ and/or $p27^{KIP1}$ or other major CKIs still develop normally, with proper differentiation, which calls the current view into question (3, 13). Although there is evidence for $p57^{KIP2}$ being involved in the differentiation of some cells (28, 30), no one has identified cell cycle factors that are controlled by differentiation signals and that critically influence the differentiation commitment process.

* Corresponding author. Mailing address: Department of Biochemistry and Molecular Biology, Graduate School and Faculty of Medicine, University of Tokyo, 7-3-1 Hongo, Bunkyo, Tokyo 113-0033, Japan. Phone: 81-3-5841-3440. Fax: 81-3-3815-1490. E-mail: okayama-tky@umin.ac.jp.

Since in lower eukaryotes the control of the cell cycle factors driving the onset of S phase greatly influences the commitment to cell differentiation, we reinvestigated the possibility of the crucial participation of some cell cycle start factors in mammalian cell differentiation control as well, using BMP-2-induced osteoblast differentiation as a model system, and we found that upon BMP-2 treatment, Cdk6 expression was down-regulated primarily by BMP-2/Smad signal-invoked transcriptional repression and that its down-regulation was essential for efficient osteoblast differentiation.

MATERIALS AND METHODS

Reagents and antibodies. Recombinant human BMP-2 was generously provided by Yamanouchi Pharmaceutical Co., Ltd. (Tokyo, Japan), and recombinant human fibroblast growth factor 2 (FGF-2) was provided by Kaken Pharmaceutical Co., Ltd. (Chiba, Japan). Antibodies against Cdk2 (H-298), Cdk4 (C-22), Cdk6 (C-21), Rb (C-15), cyclin D1 (C-20), cyclin D2 (M-20), cyclin D3 (C-16), cyclin E (M-20), p18 (M-20), p21 (H164), p27 (F-8), BMPRIA (E-16), BMPRII (T-18), and Smad6 (S-20) were obtained from Santa Cruz Biotechnology. Anti-phosphorylated Rb (G3-245) and anti-β-actin (AC-15) antibodies were purchased from Pharmingen and Sigma, respectively.

Osteoblast culture. The mouse osteoblast cell line MC3T3-E1 was purchased from the Riken Cell Bank (Tsukuba, Japan). Primary osteoblasts were isolated from neonatal mouse calvariae according to international and university guidelines (33). Calvariae dissected from 1- to 4-day-old mice were digested for 10 min with 1 ml of trypsin-EDTA (Sigma) containing 10 mg of collagenase (type 7; Sigma), and the released cells were collected. This step was repeated five times, and the cells obtained by the second through fifth digestion steps were pooled as primary osteoblasts. MC3T3-E1 cells and primary osteoblasts were maintained in α-modified minimum essential medium (α-MEM) (Life Technologies Inc.) containing 10% fetal bovine serum (FBS) (Sigma). The cells were inoculated at 5×10^4 cells in a six-well plate or 5×10^5 cells in a 10-cm-diameter plate and allowed to proliferate for 20 to 24 h, and then their growth was arrested by incubation for 24 to 48 h in α-MEM containing 0.5% FBS. Growth-arrested cells were then induced for differentiation or proliferation by stimulation with α-MEM containing 10% FBS and BMP-2 (300 ng/ml) or FGF-2 (10 nM). To block protein degradation, we added the proteasome inhibitor MG132 (*Z*-Leu-Leu-Leu-aldehyde; Peptide Institute, Osaka, Japan) to the culture medium to a final concentration of 2 μM, as described previously (15, 24).

Construction of cell clones constitutively expressing Cdk6. MC3T3-E1 cells were inoculated at 5×10^5 cells per 6-cm-diameter plate, incubated for 24 h, and then transfected with the pEF/neo I vector carrying a human *Cdk6* cDNA or no insert by use of the Lipofectamine reagent (Life Technologies, Inc.) according to the manufacturer's instructions. Twenty-four hours later, the cells were split 1:10 to 1:100 and selected in α-MEM containing 10% FBS and 200 μg of G418 (Geneticin; Life Technologies, Inc.)/ml. Stable G418-resistant colonies were then isolated and expanded for analysis. The levels of Cdk6 were then quantified by Western blotting to identify several high- and low-expression-level clones for in-depth analysis.

Smad6 expression and differentiation induction. MC3T3-E1 cells were inoculated at 5×10^4 cells per well in a six-well plate and incubated at 37°C for 20 h in α-MEM containing 10% FBS. The cells were then infected for 2 h with a recombinant adenovirus carrying *smad6* or *lacZ* at a multiplicity of infection of 100 PFU/cell, for which >80% of the cells were infected, as determined by staining for β-galactosidase. The cells were washed twice with phosphate-buffered saline (PBS), their growth was arrested by incubation in α-MEM containing 0.5% FBS for 48 h, and they were stimulated with α-MEM containing 10% FBS with or without BMP-2 (300 ng/ml).

Western blot analysis. The cells were rinsed with ice-cold PBS and lysed with RIPA buffer (10 mM Tris-HCl [pH 7.5], 150 mM NaCl, 1% Nonidet P-40 [NP-40], 0.1% sodium dodecyl sulfate [SDS], 10 μg of aprotinin/ml, 0.1 M NaF, 2 mM Na_3VO_4, and 10 mM β-glycerophosphate). After a brief sonication, the lysed cells were centrifuged at 15,000 × *g* for 20 min at 4°C to obtain soluble cell extracts. The cell extracts (10 μg of protein each) were separated by SDS–7.5, 10, or 12.5% polyacrylamide gel electrophoresis and electrotransferred to polyvinylidene difluoride membranes (Immobilon-P; Millipore Corp., Bedford, Mass.). After the blocking of nonspecific binding by soaking of the filters in 5% skim milk, the desired proteins were immunodetected with their respective antibodies, followed by visualization by use of the ECL Plus Western blotting detection system (Amersham Pharmacia Biotech, Buckinghamshire, United Kingdom) according to the manufacturer's instructions.

In vitro kinase assay. Cells were lysed with ice-cold IP buffer containing 50 mM HEPES (pH 7.5), 150 mM NaCl, 1 mM EDTA, 2.5 mM EGTA, 1 mM dithiothreitol, 0.1% Tween 20, 10% glycerol, 1 mM phenylmethylsulfonyl fluoride (PMSF), 10 μg of aprotinin/ml, 1 mM NaF, and 0.1 mM sodium orthovanadate. The lysates were incubated at 4°C for 2 h with 0.5 μg of the anti-Cdk4 or -Cdk6 antibody. Protein G-Sepharose (15 μl) (Amersham-Pharmacia) was then added and incubated for an additional 1 h. Immune complexes bound to protein G-Sepharose were precipitated by centrifugation and washed with glycerol-free IP buffer. The immunopurified Cdk4 or Cdk6 protein was incubated at 30°C for 30 min in R buffer (50 mM HEPES [pH 7.5], 2.5 mM EGTA, 10 mM KCl, 10 mM $MgCl_2$, 1 mM dithiothreitol) containing 0.5 μg of truncated Rb (Santa Cruz) and 10 mM ATP. The reaction products were electrophoresed in SDS–10% polyacrylamide gels and transferred to polyvinylidene difluoride membrane filters. Phosphorylated truncated Rb was detected with an anti-Ser780-phosphorylated Rb antibody (MBL).

Reverse transcription-PCR (RT-PCR). Total RNAs (1 μg) extracted from cells were reverse transcribed and amplified by PCR. The gene-specific primer pairs used were as follows: 5′-CGTGGTCAGGTTGTTTGATG-3′ and 5′-TGCGAAACATTTCTGCAAAG-3′ for Cdk6, 5′-ATGAGGACCCTCTCTCTGCT-3′ and 5′-CCGTAGATGCGTTTGTAGGC-3′ for osteocalcin, 5′-TAGCACCAGAGGATACCTTGC-3′ and 5′-AATGCTTCATCCTGTTCCAAA-3′ for BMPRIA, 5′-CAGAATCAAGAACGGCTATG-3′ and 5′-TTGTTTACGGTCTCCTGTCA-3′ for BMPRII, and 5′-CATGTAGGCCATGAGGTCCACCAC-3′ and 5′-TGAAGGTCGGTGTGAACGGATTTGGC-3′ for glyceraldehyde-3-phosphate dehydrogenase. The cycling parameters were 30 s at 94°C, 30 s at 55°C, and 1 min 30 s at 72°C for Cdk6, osteocalcin, and glyceraldehyde-3-phosphate dehydrogenase; and 30 s at 94°C, 30 s at 53°C, and 1 min 30 s at 72°C for BMPRIA and BMPRII.

ALP activity measurement and in situ staining. MC3T3-E1 cells were inoculated at 5×10^4 cells per well in a six-well plate and cultured in α-MEM containing 10% FBS with or without BMP-2 (300 ng/ml). After being cultured for 3 days, the cells were rinsed with PBS and lysed by sonication in 10 mM Tris-HCl buffer (pH 8.0) containing 1 mM $MgCl_2$ and 0.5% Triton X-100. The alkaline phosphatase (ALP) activity in the lysates was measured by the hydrolysis of *p*-nitrophenyl phosphate to *p*-nitrophenol. The protein content was determined by using a protein assay kit (Bio-Rad). For in situ ALP staining, the cells were fixed with 3.7% (vol/vol) formaldehyde in PBS and were stained with naphthol AS-MX phosphate (Sigma), with *N,N*-dimethyl formamide as a substrate and Fast BB salt (Sigma) as a coupler.

BrdU incorporation assay. MC3T3-E1 cells were inoculated at 10^3 cells per well in a 96-well plate and cultured in α-MEM containing 10% FBS with or without BMP-2 (300 ng/ml). After being cultured for 1 or 3 days, the cells were labeled with bromodeoxyuridine (BrdU) for 2 h, and the cell population entering S phase was determined by quantifying the incorporated BrdU (Cell Proliferation ELISA; Roche Molecular Biochemical, Mannheim, Germany).

XTT assay. Cells were inoculated at 10^3 cells per well in a 96-well plate and cultured for 5 days in α-MEM containing 10% FBS with or without BMP-2 (300 ng/ml), with cell sampling every day. The sampled cells were quantified by use of an XTT {sodium 3,3-[(phenylamino)carbonyl]-3,4-tetrazolium-bis(4-methoxy-6-nitro) benzenesulfonic acid hydrate} assay kit (Roche).

Flow cytometric analysis. Approximately 10^5 cells were suspended in 0.02 ml of citrate buffer and subjected to the following serial treatments at room temperature: (i) the addition of 0.18 ml of solution A (0.03 mg of trypsin/ml, 3.4 mM trisodium citrate, 0.1% NP-40, 1.5 mM spermine 4HCl, and 0.5 mM Tris-HCl [pH 7.6]) and incubation for 10 min; (ii) the addition of 0.15 ml of solution B (3.4 mM trisodium citrate, 0.1% NP-40, 1.5 mM spermine-4HCl, 0.5 mM Tris-HCl [pH 7.6], 0.5 mg of trypsin inhibitor/ml, 0.1 mg of RNase A/ml) and incubation for 10 min; and (iii) the addition of 0.15 ml of solution C (4.16 mg of propidium iodide/ml, 3.4 mM trisodium citrate, 0.1% NP-40, 4.8 mM spermine 4HCl, 0.5 mM Tris-HCl [pH 7.6]) and incubation for 10 min. The DNA content was determined and analyzed with EPICS XL and XL EXPO32 instruments (Beckman).

ChIP. Chromatin immunoprecipitation (ChIP) was performed by use of a commercial kit (Upstate Cell Signaling Solutions, Lake Placid, N.Y.). Cells were inoculated at a density of 5×10^5 cells per 10-cm-diameter dish and cultured in α-MEM containing 10% FBS and BMP-2 (300 ng/ml). At days 1 and 4 of culture, the protein and DNA were cross-linked by the direct addition of formaldehyde to the culture medium to a final concentration of 1% and incubation at 37°C for 10 min. The cells were then washed twice with ice-cold PBS containing 1 mM PMSF and 1 μg of aprotinin/ml, collected with cell scrapers, sedimented by low-speed centrifugation, resuspended, and incubated at 4°C for 10 min in 200 μl

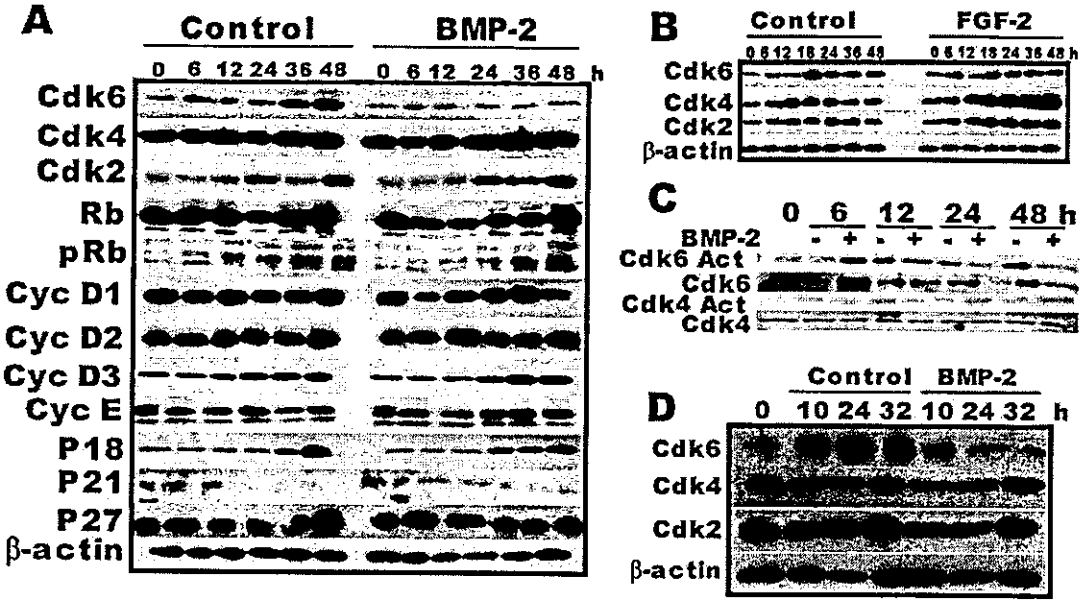

FIG. 1. BMP-2 treatment inhibits expression of Cdk6. (A) Time-dependent expression of cell cycle factors controlling the G_1-S transition in mouse osteoblastic MC3T3-E1 cells during differentiation induction. Growth-arrested MC3T3-E1 cells were stimulated with FBS in the presence or absence of BMP-2, with cell sampling done at the indicated times. The amounts of cell cycle factors expressed during stimulation were semiquantified by Western blotting. β-Actin was used as a loading control. Cyc, cyclin. (B) Time-dependent expression of Cdks 2, 4, and 6 in MC3T3-E1 cells during FGF-2 stimulation. Growth-arrested MC3T3-E1 cells were stimulated with FBS in the presence or absence of FGF-2, with cell sampling performed at the indicated times, followed by Western blotting of Cdks 2, 4, and 6. (C) Cdk6 and Cdk4 activities in MC3T3-E1 cells during stimulation with or without BMP-2. Cdk6 and Cdk4 were immunoprecipitated and assayed for kinase activity, and their amounts were determined in parallel. (D) Time-dependent expression of Cdk2, Cdk4, and Cdk6 proteins in primary neonatal mouse calvarial osteoblasts stimulated with or without BMP-2.

of lysis buffer (1% SDS, 10 mM EDTA, 50 mM Tris [pH 8.1]) containing 1 mM PMSF and 1 μg of aprotinin/ml. The cell lysates were then sonicated at 4°C with a Branson 450 sonifier at an output control of 2 and a duty cycle of 10 for 10 s to fragment the chromosomal DNA into 0.2- to 1-kb pieces. After the insoluble material was removed by centrifugation at 15,000 × *g* for 10 min, 1/10 aliquots of the supernatants were taken and saved as input. The rest of the supernatants were diluted appropriately with ChIP dilution buffer (0.01% SDS, 1.1% Triton X-100, 1.2 mM EDTA, 16.7 mM Tris-HCl [pH 8.1], 167 mM NaCl) containing 1 mM PMSF and 1 μg of aprotinin/ml and were pretreated with a salmon sperm DNA-protein A–50% agarose slurry at 4°C for 30 min with gentle agitation. After a brief centrifugation to remove the slurry, the supernatants were collected and incubated at 4°C overnight with antibodies (anti-mouse pRb [1 μg each of Ab-4 and Ab-5; Neomarkers] or anti-CBFA1 [2 μg of sc-8566; Santa Cruz]). Immunocomplexes were allowed to bind to protein A-agarose by incubation with a salmon sperm DNA–protein A–50% agarose slurry at 4°C for 1 h with gentle agitation. After a brief centrifugation, the supernatants were saved as the unbound fraction. The protein A-bound immunocomplexes were washed once with 1 ml each of the buffers shown below in sequential order: (i) low-salt immune complex wash buffer (0.1% SDS, 1% Triton X-100, 2 mM EDTA, 20 mM Tris-HCl [pH 8.1], 150 mM NaCl), (ii) high-salt immune complex wash buffer (0.1% SDS, 1% Triton X-100, 2 mM EDTA, 20 mM Tris-HCl [pH 8.1], 500 mM NaCl), (iii) LiCl immune complex wash buffer (0.25 M LiCl, 1% IGEPAL-CA630, 1% sodium deoxycholate, 1 mM EDTA, 10 mM Tris, pH 8.1), and (iv) TE buffer (10 mM Tris-HCl, 1 mM EDTA, pH 8.0). The protein A-bound immunocomplexes were resuspended in 250 μl of elution buffer (1% SDS, 0.1 M $NaHCO_3$), mixed by vortexing, and incubated at room temperature for 15 min, with gentle agitation. After a brief centrifugation, the supernatants were saved, and elution was repeated one more time. Both eluates were combined, and after the addition of 20 μl of 5 M NaCl, were heated at 65°C for 4 h to reverse cross-linking. Ten microliters of 0.5 M EDTA, 20 μl of 1 M Tris-HCl (pH 6.5), and 2 μl of proteinase K (20 mg/ml) were added to the eluates, and the mixtures were incubated for 1 h at 45°C to remove proteins bound to DNA, followed by sequential extraction steps with phenol-chloroform and chloroform and by DNA precipitation with ethanol after the addition of 10 μg of glycogen as a carrier. The precipitated DNA was recovered by centrifugation and resuspended in 100 μl of TE buffer. The input fractions of the supernatants and the unbound fractions were similarly treated to remove cross-links and proteins, and the DNAs were ethanol precipitated similarly and dissolved in 10 and 100 μl of TE buffer, respectively. The osteocalcin and myogenin promoter sequences were amplified by 40 cycles of PCR from 1 μl each of the DNA solutions, with parameters of 30 s at 95°C, 30 s at 60°C, and 30 s at 72°C and with the following primers: 5′-CTGAACTGGGCAAATGAGGACA-3′ and 5′-AGGGGATGCT GCCAGGACTAAT for the mouse osteocalcin promoter (positions −67 to −471) and 5′-ACCCCTTTCTTGTTCCCTTCCT-3′ and 5′-CTCCCGCAGCC CCTCAC-3′ for the mouse myogenin promoter (positions −9 to −431).

Statistical analysis. The means of groups were compared by analysis of variance, and the significance of differences was determined by post hoc testing using the Bonferroni method.

RESULTS

Cdk6 is down-regulated in osteoblasts upon BMP-2 treatment. Within 24 h after treatment with BMP-2, C2C12 cells begin to express osteocalcin mRNA and ALP, two representative markers of mature osteoblasts (21). Accordingly, the commitment to BMP-2-induced osteoblast differentiation occurs within 24 h. Since the MC3T3-E1 cells used in the present study are known to be in a stage that is one step more differentiated toward mature osteoblasts than C2C12 cells, we assumed that the commitment of this cell line to BMP-2-induced osteoblast differentiation occurred well within 24 h, and therefore we analyzed the effect of BMP-2 on the initial 48-h expression levels of cell cycle factors that critically regulate the onset of S phase in this cell line. The cells were arrested in quiescence by serum starvation, stimulated with serum in the presence or absence of BMP-2, and harvested every 6 or 12 h. The amounts of cyclins (D1, D2, D3, and E), Cdk2, Cdk4,

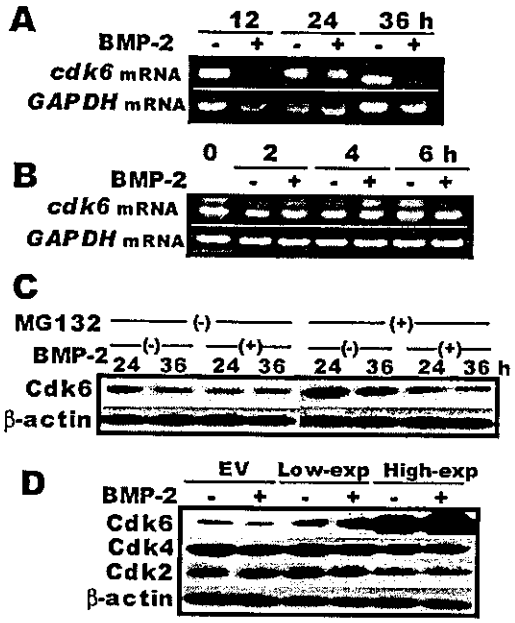

FIG. 2. BMP-2 down-regulates Cdk6 expression mainly via preventing transcription. (A) BMP-2 treatment markedly reduces *cdk6* mRNA level. Growth-arrested MC3T3-E1 cells were stimulated with or without BMP-2 for the indicated times, and RNAs were prepared. *cdk6* mRNA was semiquantified by RT-PCR. (B) BMP-2 treatment does not affect the stability of *cdk6* mRNA. Growth-arrested MC3T3-E1 cells were stimulated with serum for 6 h and then incubated with actinomycin D (Sigma) (0.1 μg/ml) with or without the addition of BMP-2. RNAs were prepared and the Cdk6 transcript was semiquantified by RT-PCR. Glyceraldehyde-3-phosphate dehydrogenase (GAPDH) mRNA was used as a control for the RNA preparations. (C) The proteasome inhibitor MG132 does not influence the action of BMP-2 on the Cdk6 protein level. Growth-arrested MC3T3-E1 cells were stimulated for 24 and 36 h with or without BMP-2 and/or MG132 (2 μM), and the Cdk6 protein levels were determined by Western blotting. (D) BMP-2 treatment does not affect the level of forcefully expressed Cdk6 protein. Clones constitutively expressing Cdk6 from an EF1α-promoter as well as empty vector-transfected MC3T3-E1 (EV) cells were growth arrested as described in the text and stimulated for 48 h with or without BMP-2. The amounts of Cdk6, Cdk4, and Cdk2 were then semiquantified by Western blotting.

Cdk6, CKIs (p18, p21, p27, and p57), and Rb and phosphorylated Rb proteins in the whole-cell lysate at each time point were analyzed by Western blotting (Fig. 1). In this cell line, the amounts of Cdk6, Cdk2, and p18 increased during serum stimulation, as early as 6 h after stimulation, and the amount of p21 decreased, whereas the amounts of the remaining factors were unchanged. This cell line did not express detectable amounts of p57 throughout the experiment (data not shown). Coinciding with the elevation of Cdk2, phosphorylated forms of the Rb protein appeared. Under these conditions, the cells grew to confluence but did not commit to differentiation into osteoblasts.

In contrast, when MC3T3-E1 cells were stimulated with BMP-2 to stimulate osteoblast differentiation, the induction of Cdk6 completely disappeared (Fig. 1A), while the levels of the remaining factors, including Cdk4, were virtually indistinguishable from those obtained by serum stimulation. The behavioral difference between Cdk6 and Cdk4 was further noticeable in another experiment. When MC3T3-E1 cells were treated with FGF-2, a potent stimulator of osteoblast proliferation, the level of Cdk4, but not that of Cdk6, was markedly elevated (Fig. 1B).

To confirm that the blocked induction of Cdk6 was faithfully reflected by its kinase activities, we assayed the activities of Cdk6 and Cdk4 during serum stimulation in the presence and absence of BMP-2. When the cells were stimulated with serum, Cdk6 activity increased at 12 h and remained high at least until 48 h. In contrast, when the cells were stimulated with serum containing BMP-2, Cdk6 activity increased at 6 h, but rapidly decreased to the basal level by 12 and 24 h, the times expected for the commitment to differentiation to take place (Fig. 1C). These activities were roughly correlated with the amounts of immunoprecipitated Cdk6, which faithfully reflected its amounts in whole-cell lysates (Fig. 1A), except for the BMP-2-treated 6-h sample, from which Cdk6 was more efficiently immunoprecipitated. This result was reproducible, but its reason was unclear.

On the other hand, there was no significant difference in the time course and extent of Cdk4 activation between BMP-2-treated and untreated MC3T3-E1 cells. Thus, despite the fact that Cdk4 and Cdk6 are structurally homologous (11) and share D cyclins as their catalytic partners, only the expression of Cdk6 was significantly influenced by BMP-2 treatment. We did a similar experiment with proliferating MC3T3-E1 cells and observed a similar down-regulation of Cdk6 upon BMP-2 treatment, although it was less obvious, perhaps due to the lack of synchronization in their cell cycle progression (data not shown).

Cdk6 down-regulation is not specific to this cell line and is a more general phenomenon. We performed the same Western blot analysis with a culture of primary osteoblasts isolated from neonatal mouse calvariae and obtained the same results. Treatment with BMP-2 during serum stimulation completely blocked the induction of Cdk6 at 24 and 32 h, whereas Cdk4 and Cdk2 were uninfluenced (Fig. 1D). These results show that Cdk6 was specifically down-regulated during the commitment to BMP-2-induced osteoblast differentiation.

BMP-2-led Cdk6 down-regulation is exerted at the transcriptional level. We performed a semiquantitative RT-PCR analysis of the Cdk6 transcript and found that *cdk6* mRNA disappeared when MC3T3-E1 cells were stimulated with BMP-2 (Fig. 2A). In contrast, BMP-2 did not significantly influence the stability of either *cdk6* mRNA or protein. When the cells were stimulated with serum for 6 h and then treated with

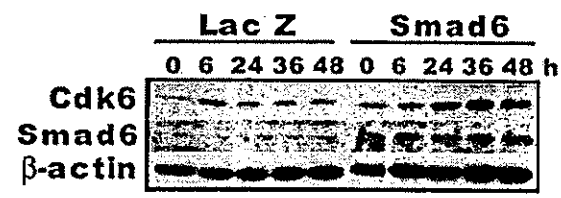

FIG. 3. Smad6 overexpression effectively blocks BMP-2-led down-regulation of Cdk6. MC3T3-E1 cells were infected with a recombinant adenovirus carrying the *smad6* or *lacZ* gene and were subsequently growth arrested by incubation in a low-serum-level medium for 48 h. The cells were then stimulated with serum in the presence or absence of BMP-2. The expression of Cdk6 and Smad6 was determined by Western blotting, with β-actin used as a loading control.

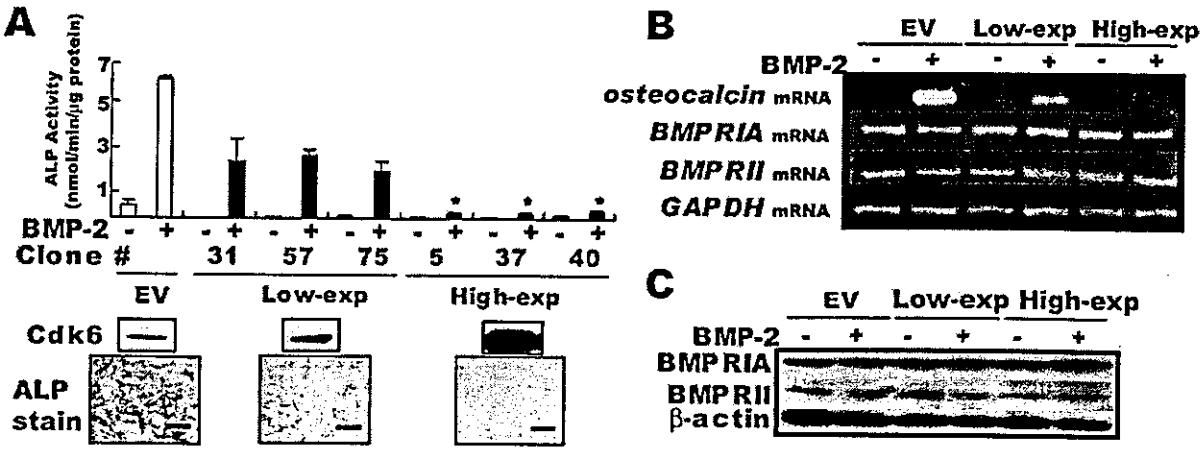

FIG. 4. Overexpression of Cdk6 inhibits BMP-2-induced osteoblast differentiation. MC3T3-E1 cell clones expressing low (no. 31, 57, and 75) or high (no. 5, 37, and 40) levels of Cdk6 and empty vector-transfected MC3T3-E1 (EV) cells were induced for osteoblast differentiation by treatment with BMP-2 according to the standard protocol. (A) After 72 h of treatment, the induced ALP activity was assayed (top). The middle panel shows Western blot data for Cdk6 in growing empty vector-transfected cells and cells from clones 31 and 40. *, $P < 0.1$; there is a significant difference from the ALP activity of BMP-2-treated empty vector-transfected cells. The bottom panels show ALP staining of empty vector-transfected cells and clones 31 and 40. Bars, 100 μm. (B) Levels of osteocalcin, BMPRIA, and BMPRII mRNAs, as determined by semiquantitative RT-PCRs with empty vector-transfected cells and clones 31 and 40 stimulated for 48 h with or without BMP-2. GAPDH mRNA was used as a control for the RNA preparations. (C) Protein levels of BMPRIA and BMPRII in empty vector-transfected cells and clones 31 and 40 stimulated for 48 h with or without BMP-2.

actinomycin D in the presence or absence of BMP-2, there was no difference in the rate of disappearance of the Cdk6 transcript between the treatment and nontreatment groups (Fig. 2B).

Cdk4 is known to be degraded by the ubiquitin-proteasome system (27). Because Cdk6 and Cdk4 are siblings and execute similar functions, we assumed that Cdk6 was likely to be degraded by the same proteolytic system. When MC3T3-E1 cells were treated with MG132, a potent inhibitor of this proteolytic system, during serum stimulation in the absence of BMP-2, the level of Cdk6 was elevated two- to threefold, consistent with this assumption (Fig. 2C). In the presence of BMP-2, MG132 treatment elevated the level of Cdk6 by the same degree, suggesting that there is no acceleration of Cdk6 degradation by treatment with this differentiation inducer. To further confirm that BMP-2 did not affect the stability of the Cdk6 protein, we constructed and analyzed MC3T3-E1 cell clones that constitutively expressed Cdk6 at low and high levels. BMP-2 treatment did not influence the levels of Cdk6 protein expressed from the constitutive EF1α promoter (Fig. 2D). These findings indicate that BMP-2 down-regulates Cdk6 expression mainly, if not exclusively, by transcriptional repression.

Smads mediate BMP-2-induced down-regulation of Cdk6. A differentiation signal invoked by BMP-2 is known to be mediated by Smad proteins, particularly R-Smads and Co-Smads, while I-Smads, such as Smad6 and Smad7, inhibit this signaling (6). To investigate whether Smads mediate Cdk6 down-regulation, we overexpressed Smad6 in MC3T3-E1 cells by use of an adenovirus vector and examined its effect on BMP-2-led Cdk6 down-regulation. As shown in Fig. 3, BMP-2-led Cdk6 down-regulation was completely abolished by the overexpression of Smad6, indicating that Smads do indeed mediate the BMP-2-led Cdk6 down-regulation.

Osteoblasts overexpressing Cdk6 strongly resist BMP-2-invoked differentiation. As discussed above, Cdk6 was down-regulated during BMP-2-invoked osteoblast differentiation. Consequently, a key question is whether this down-regulation is essential for osteoblast differentiation or not. To address this question, we constructed >100 MC3T3-E1 cell clones that stably expressed various levels of Cdk6 by transfecting MC3T3-E1 cells with an expression vector harboring *Cdk6* cDNAs and then tested their ability to respond to BMP-2 and to differentiate into mature osteoblasts. Figure 2D shows the protein levels of Cdk6, Cdk4, and Cdk2 in some representative clones that were treated with BMP-2 or were left untreated compared to the protein levels in similarly treated empty vector-transfected control MC3T3-E1 cells. The Cdk4 and Cdk2 protein levels were not affected by the overexpression of Cdk6, suggesting the absence of any particular compensatory regulation of Cdk4 or Cdk2 expression upon Cdk6 overexpression.

The ability of BMP-2 to induce osteoblast differentiation, as monitored by ALP production and osteocalcin expression, which are well-characterized early and late differentiation markers, respectively, was then studied with control cells and low (~2-fold) and high (>10-fold) Cdk6 expressers. The induction of ALP upon BMP-2 treatment was inhibited significantly in the low expressers and completely in the high expressers (Fig. 4A). Osteocalcin mRNA, as measured by semiquantitative RT-PCR, was markedly reduced in the low expressers and was undetectable in the high expressers (Fig. 4B). Thus, a twofold overexpression of Cdk6, or the same level of exogenous Cdk6 expression as endogenous expression, already showed a strong inhibitory effect on differentiation. This implies that the presence of the original level of Cdk6 expression was enough to markedly inhibit the BMP-2-invoked differentiation of MC3T3-E1 cells.

TABLE 1. Proliferation and cell cycle distribution of MC3T3-E1 cells that overexpress Cdk6[a]

Cell type	BrdU incorporation (OD) at indicated time (h) in presence or absence of BMP-2				Flow cytometric analysis result in presence or absence of BMP-2			
	24		72		% G_0/G_1		%G_2/M	
	−	+	−	+	−	+	−	+
Empty vector	0.37 ± 0.01	0.37 ± 0.12	0.07 ± 0.01	0.08 ± 0.01	78 ± 0	80 ± 1	16 ± 1	15 ± 0
Low expresser	0.41 ± 0.05	0.37 ± 0.08	0.06 ± 0.02	0.08 ± 0.02	78 ± 1	76 ± 0	17 ± 1	18 ± 1
High expresser	0.55 ± 0.07	0.43 ± 0.07	0.05 ± 0.01	0.06 ± 0.01	77 ± 0	79 ± 1	15 ± 1	15 ± 1

[a] Cell proliferation was determined by BrdU incorporation after 24 and 72 h of culture in the presence and absence of BMP-2. Cell cycle distribution was determined by flow cytometric analysis of cells after 24 h of culture. Three representative clones (31, 57, and 75 and 5, 37, and 40, respectively) were chosen from the low- and high-expressing group. Data are expressed as means ± standard deviations after analysis of cells in eight separate wells for each clone.

The Cdk6-led resistance to osteoblast differentiation is unlikely to be caused by an unexpected interference of the BMP-2/Smads signaling pathway by the overexpressed Cdk6. Neither the mRNA nor the protein levels of the BMP receptors BMPRIA and BMPRII were significantly affected by Cdk6 expression (Fig. 4B and C).

Overexpression of Cdk6 does not influence proliferation of osteoblasts. Because Cdk6 promotes the G_1-S transition, the suppression of osteoblast differentiation by overexpressed Cdk6 could be a mere consequence of its execution of this role. We therefore examined the effects of both BMP-2 and Cdk6 overexpression on the G_1-S transition and the proliferation of MC3T3-E1 cells. Empty vector-transfected MC3T3-E1 cells, as well as the low and high Cdk6 expressers, were similarly arrested in quiescence, stimulated with serum in the presence or absence of BMP-2, and analyzed for S-phase entry as well as for cell populations in G_0-G_1 and G_2-M by BrdU incorporation and flow cytometric analyses (Table 1). Cell proliferation was also monitored in the presence and absence of BMP-2 by an XTT assay (Fig. 5). The overexpression of Cdk6 did not cause any significant changes in either the cell cycle distribution or the proliferation rate of the cells, regardless of whether the cells were stimulated with BMP-2 or not. These results suggest that the inhibitory effect of Cdk6 on osteoblast differentiation is not exerted via cell cycle regulation.

The Cdk6-exerted differentiation block is correlated with a loss of the binding of Runx2/Cbfa1, but not Rb, to the osteocalcin promoter. Rb, a potent repressor of the E2F-DP transcriptional factor that is essential for the onset of S phase, has been reported to also act as a transcriptional coactivator for Runx2/Cbfa1, a key transcriptional factor for osteoblast differentiation (23). Since Rb is a direct target of Cdk6 for cell cycle control, we examined whether Rb mediates the Cdk6-exerted inhibition of osteoblastic differentiation by determining the effects of overexpressed Cdk6 on the vivo binding of Runx2/Cbfa1 and Rb to the osteocalcin promoter during BMP-2 treatment. To this end, we performed a ChIP assay. The specificities of the anti-Runx2/Cbfa1 and anti-Rb antibodies used for this assay were confirmed by the lack of precipitation of the irrelevant myogenin promoter, but the clear precipitation of the osteocalcin promoter, by both antibodies (Fig. 6).

Using these antibodies, we compared the binding levels of Runx2/Cbfa1 and Rb to the osteocalcin promoter in empty vector-transfected MC3T3-E1 cells and in low and high Cdk6 expressers at day 1 (a time just after the differentiation commitment) and day 4 (well after the onset of full differentiation phenotypes for MC3T3-E1 cells) post-BMP-2 treatment. As shown in Fig. 6A, on day 1 Runx2/Cbfa1 bound slightly to the osteocalcin promoter in the empty vector-transfected MC3T3-E1 cells, but not in either the low or high Cdk6 expressers, whereas no binding of Rb to this promoter was detected in any of these cells. On day 4, when osteocalcin was fully expressed, the binding of Runx2/Cbfa1 to this promoter was clearly detected in the empty vector-transfected MC3T3-E1 cells and the low Cdk6 expresser, but not in the high Cdk6 expresser, in which osteoblast differentiation was completely blocked (Fig. 4) despite a high level of Runx2/Cbfa1 expression (Fig. 6B). Thus, there was a close correlation between osteoblast differentiation and the binding of Runx2/Cbfa1 to the osteocalcin promoter in Cdk6-led differentiation inhibition. In

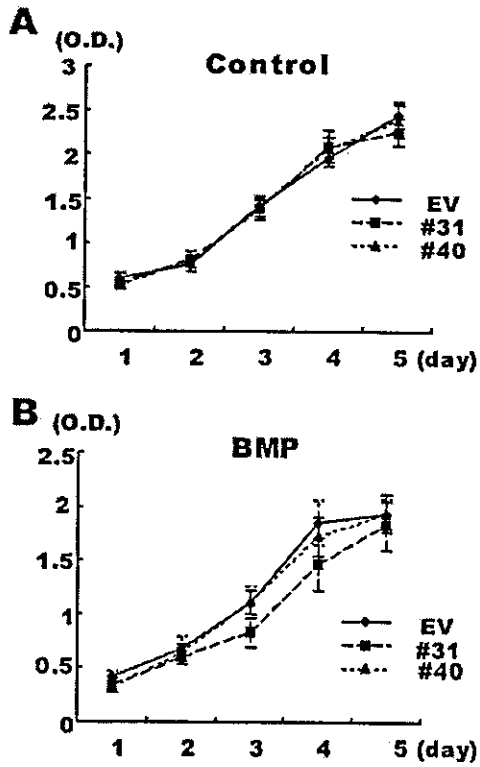

FIG. 5. Overexpression of Cdk6 does not influence proliferation of MC3T3-E1 cells. Proliferation rates were determined by XTT staining of empty vector-transfected cells (EV) and clones 31 and 40 cultured in the presence (B) or absence (A) of BMP-2, with cell sampling done every day.

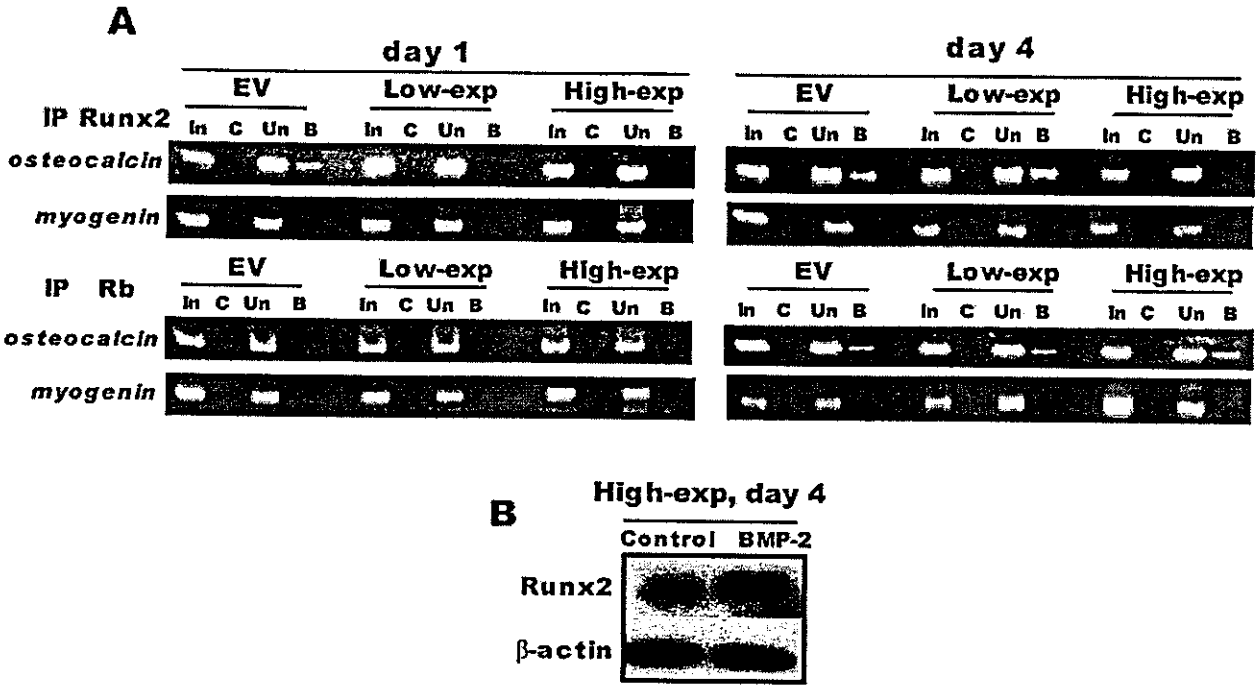

FIG. 6. Cdk6-exerted differentiation block is correlated with a loss of binding of Runx2/Cbfa1, but not Rb, to the osteocalcin promoter. (A) ChIP assay performed with empty vector-transfected MC3T3-E1 cells (EV) and clones 31 (low Cdk6 expresser) and 40 (high Cdk6 expresser) cultured for 1 and 4 days with BMP-2, as described in Materials and Methods. IP Rb, immunoprecipitation with an anti-Rb antibody; IP Runx2, immunoprecipitation with an anti-Runx2/Cbfa1 antibody; In, total DNA input for each sample; C, immunoprecipitation with control serum; Un, PCR from the supernatant after immunoprecipitation; B, PCR from immunoprecipitation product. The primer sets for PCRs of the osteocalcin and myogenin promoter regions are described in Materials and Methods. (B) Runx2/Cbfa1 is expressed in a high Cdk6 expresser cultured for 4 days with or without BMP-2. The level of Runx2/Cbfa1 was determined by Western blotting. The loading control is β-actin.

contrast, there was no apparent correlation between Rb binding and osteoblastic differentiation. On day 4, the binding of Rb to the osteocalcin promoter was detected, as reported previously (23), but it was present in all of the cells, despite the fact that osteoblastic differentiation in the high Cdk6 expresser was completely blocked. Moreover, Rb seemed to bind the promoter independently of Runx2/Cbfa1, because in the high Cdk6 expresser, Rb bound the promoter without the binding of Runx2/Cbfa1.

These ChIP assay results indicate that Rb is unlikely to mediate the Cdk6-led differentiation inhibition, although it is certainly required for the efficient osteoblast differentiation of MC3T3-E1 cells (23). In addition, the loss of Runx2/Cbfa1 binding to the osteocalcin promoter during Cdk6-exerted differentiation inhibition raises the possibility that Cdk6 may inhibit osteoblastic differentiation by blocking the promoter-binding ability of the Runx2/Cbfa1 transcriptional factor.

DISCUSSION

In the present study, we have shown that Cdk6 expression is shut down mainly at transcription upon BMP-2 treatment and that this shutdown, mediated by BMP-2-activated Smad signaling, is required for efficient osteoblast differentiation. Osteoblastic cells, including the presently used MC3T3-E1 cell line and primary mouse osteoblasts, express both Cdk4 and Cdk6, yet only Cdk6 is critically involved in the commitment to dif-

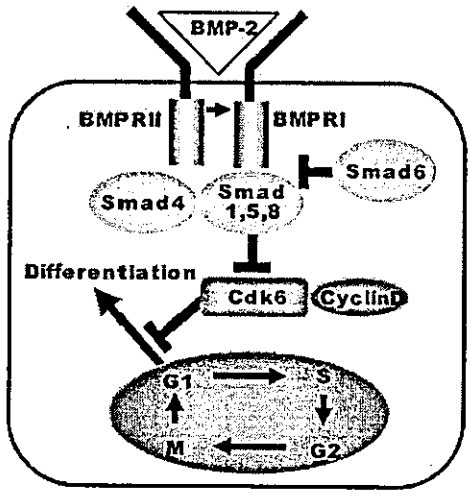

FIG. 7. Schematic presentation of the mechanism by which Cdk6 inhibits osteoblastic differentiation. BMP-2 binds the type II receptor, which subsequently activates the type I receptor by direct association. The activated type I receptor directly phosphorylates R-Smads (Smads 1, 5, and 8) and promotes their complex formation with Co-Smad (Smad4). The R-Smads/Co-Smad complexes are then translocated into the nucleus, where they repress the transcription of the *cdk6* gene and permit osteoblastic differentiation to take place.

ferentiation. This study demonstrates that Cdk6 is a key molecule determining the differentiation rate of osteoblasts as a downstream effector of BMP-2/Smad signaling. Figure 7 depicts a schematic presentation of the mechanism by which BMP-2 induces osteoblast differentiation, as revealed by the present and previous studies. BMP-2 binds to the type II receptor and activates the type I receptor, leading to the formation of R-Smads/Co-Smad complexes, which are imported into the nucleus. The R-Smads/Co-Smad complexes then repress the *cdk6* promoter, thereby removing Cdk6-exerted blocking of differentiation.

The Cdk6-cyclin D3 complex is unique among cyclin D-cognate kinase combinations and evades inhibition by CKIs (8). Therefore, it can greatly enhance the proliferative potential of fibroblasts under growth-suppressive conditions and consequently sensitizes cells to physical and chemical transformation (2). This unique ability of Cdk6, however, does not seem to be responsible for the requirement of Cdk6 down-regulation for efficient osteoblast differentiation because we did not find any noticeable effect of BMP-2 and Cdk6 overexpression on the proliferation or even the cell cycle progression of MC3T3-E1 cells under the experimental conditions we employed. This apparent lack of a growth-stimulating function for Cdk6 in this cell line is consistent with the observation that Cdk4, but not Cdk6, was up-regulated by FGF-2, a potent stimulator of osteoblast proliferation.

The Rb protein has been implicated in osteoblast differentiation. The incidence of osteosarcoma increases 500-fold in patients inheriting *Rb* gene mutations. Recently, the Rb protein was reported to physically interact with Runx2/Cbfa1, which transactivates osteoblast-specific promoters (23). This transactivation is lost in tumor-derived Rb protein mutants, underscoring its potential role in osteoblast differentiation. The possibility that Rb directly mediates the role of Cdk6 as a differentiation inhibitor, however, is remote because unlike for Runx2/Cbfa1, there was no apparent correlation between the Cdk6-exerted differentiation block and the binding of Rb to the osteocalcin promoter.

How could Cdk6 control differentiation without influencing cell cycling? One possibility is that Cdk6 directly controls a factor(s) that is critically involved in differentiation. This possibility may not be as remote as is generally thought. In *Schizosaccharomyces pombe*, Pas1 cyclin and its partner kinase Pef1 activate a transcriptional factor complex that is functionally equivalent to E2F-DP of mammals, thereby promoting S-phase entry, just like Cdk6, yet they independently inhibit mating pheromone signaling, whose activation is essential for the differentiation of yeast cells (22). Thus, this may be a good model for the situation of Cdk6 in BMP-2-induced osteoblast differentiation, highlighting a potential functional similarity between Cdk6 and Pef1.

This study demonstrates for the first time that Cdk6, a G_1 cell cycle factor, plays a critical role in controlling BMP-2-invoked osteoblast differentiation. Several transcription factors, such as Runx2/Cbfa1, osterix, and low-density lipoprotein receptor protein 5, have been reported to be involved in bone formation (12, 16). Consequently, one of these factors may be responsible for the BMP-2-invoked repression of Cdk6 transcription. The identification of the transcriptional repressor as well as key targets of Cdk6 will definitely be required for a deeper understanding of the molecular basis of bone formation.

Finally, it is appropriate to stress that our finding is not specific to BMP-2-induced osteoblast differentiation. Very recently, Matushansky et al. reported a similar role for Cdk6 in the erythroid differentiation of a murine leukemia cell line (10).

ACKNOWLEDGMENTS

We thank Kohei Miyazono and Takeshi Imamura for kindly providing an adenovirus vector carrying *smad6* and Izumu Saito for an adenovirus vector carrying *lacZ*. We also thank H. Chikuda, M. Tsuji, and K. Baba for helpful discussion and support.

This work was supported by grants from the Department of Science, Education and Culture of Japan.

REFERENCES

1. **Bai, S., X. Shi, X. Yang, and X. Cao.** 2000. Smad6 as a transcriptional corepressor. J. Biol. Chem. 275:8267–8270.
2. **Chen, Q., J. Lin, S. Jinno, and H. Okayama.** 2003. Overexpression of Cdk6-cyclin D3 highly sensitizes cells to physical and chemical transformation. Oncogene 22:992–1001.
3. **Deng, C., P. Zhang, J. W. Harper, S. J. Elledge, and P. Leder.** 1995. Mice lacking p21CIP1/WAF1 undergo normal development, but are defective in G1 checkpoint control. Cell 82:675–684.
4. **DiChiara, M. R., J. M. Kiely, M. A. Gimbrone, Jr., M. E. Lee, M. A. Perrella, and J. N. Topper.** 2000. Inhibition of E-selectin gene expression by transforming growth factor beta in endothelial cells involves coactivator integration of Smad and nuclear factor kappaB-mediated signals. J. Exp. Med. 192:695–704.
5. **Hinds, P. W., and R. A. Weinberg.** 1994. Tumor suppressor genes. Curr. Opin. Genet. Dev. 4:135–141.
6. **Kretzschmar, M., and J. Massague.** 1998. SMADs: mediators and regulators of TGF-beta signaling. Curr. Opin. Genet. Dev. 8:103–111.
7. **Lee, K. S., H. J. Kim, Q. L. Li, X. Z. Chi, C. Ueta, T. Komori, J. M. Wozney, E. G. Kim, J. Y. Choi, H. M. Ryoo, and S. C. Bae.** 2000. Runx2 is a common target of transforming growth factor beta1 and bone morphogenetic protein 2, and cooperation between Runx2 and Smad5 induces osteoblast-specific gene expression in the pluripotent mesenchymal precursor cell line C2C12. Mol. Cell. Biol. 20:8783–8792.
8. **Lin, J., S. Jinno, and H. Okayama.** 2001. Cdk6-cyclin D3 complex evades inhibition by inhibitor proteins and uniquely controls cell's proliferation competence. Oncogene 20:2000–2009.
9. **Lopez-Rovira, T., E. Chalaux, J. L. Rosa, R. Bartrons, and F. Ventura.** 2000. Interaction and functional cooperation of NF-kappa B with Smads. Transcriptional regulation of the JunB promoter. J. Biol. Chem. 275:28937–28946.
10. **Matushansky, I., F. Radparvar, and A. I. Skoultchi.** 2003. CDK6 blocks differentiation: coupling cell proliferation to the block to differentiation in leukemic cells. Oncogene 22:4143–4149.
11. **Meyerson, M., G. H. Enders, C. L. Wu, L. K. Su, C. Gorka, C. Nelson, E. Harlow, and L. H. Tsai.** 1992. A family of human cdc2-related protein kinases. EMBO J. 11:2909–2917.
12. **Nakashima, K., X. Zhou, G. Kunkel, Z. Zhang, J. M. Deng, R. R. Behringer, and B. de Crombrugghe.** 2002. The novel zinc finger-containing transcription factor osterix is required for osteoblast differentiation and bone formation. Cell 108:17–29.
13. **Nakayama, K., N. Ishida, M. Shirane, A. Inomata, T. Inoue, N. Shishido, I. Horii, and D. Y. Loh.** 1996. Mice lacking p27(Kip1) display increased body size, multiple organ hyperplasia, retinal dysplasia, and pituitary tumors. Cell 85:707–720.
14. **Nevins, J. R.** 1992. E2F: a link between the Rb tumor suppressor protein and viral oncoproteins. Science 258:424–429.
15. **Nishimori, S., Y. Tanaka, T. Chiba, M. Fujii, T. Imamura, K. Miyazono, T. Ogasawara, H. Kawaguchi, T. Igarashi, T. Fujita, K. Tanaka, and H. Toyoshima.** 2001. Smad-mediated transcription is required for transforming growth factor-beta 1-induced p57(Kip2) proteolysis in osteoblastic cells. J. Biol. Chem. 276:10700–10705.
16. **Patel, M. S., and G. Karsenty.** 2002. Regulation of bone formation and vision by LRP5. N. Engl. J. Med. 346:1572–1574.
17. **Reddi, A. H.** 1998. Role of morphogenetic proteins in skeletal tissue engineering and regeneration. Nat. Biotechnol. 16:247–252.
18. **Sherr, C. J.** 1994. G1 phase progression: cycling on cue. Cell 79:551–555.
19. **Sherr, C. J., and J. M. Roberts.** 1999. CDK inhibitors: positive and negative regulators of G1-phase progression. Genes Dev. 13:1501–1512.
20. **Shi, X., X. Yang, D. Chen, Z. Chang, and X. Cao.** 1999. Smad1 interacts with homeobox DNA-binding proteins in bone morphogenetic protein signaling. J. Biol. Chem. 274:13711–13717.

21. **Takeda, K., H. Ichijo, M. Fujii, Y. Mochida, M. Saitoh, H. Nishitoh, T. K. Sampath, and K. Miyazono.** 1998. Identification of a novel bone morphogenetic protein-responsive gene that may function as a noncoding RNA. J. Biol. Chem. 273:17079–17085.
22. **Tanaka, K., and H. Okayama.** 2000. A Pcl-like cyclin activates the Res2p-Cdc10p cell cycle "start" transcriptional factor complex in fission yeast. Mol. Biol. Cell 11:2845–2862.
23. **Thomas, D. M., S. A. Carty, D. M. Piscopo, J. S. Lee, W. F. Wang, W. C. Forrester, and P. W. Hinds.** 2001. The retinoblastoma protein acts as a transcriptional coactivator required for osteogenic differentiation. Mol. Cell 8:303–316.
24. **Urano, T., H. Yashiroda, M. Muraoka, K. Tanaka, T. Hosoi, S. Inoue, Y. Ouchi, and H. Toyoshima.** 1999. p57(Kip2) is degraded through the proteasome in osteoblasts stimulated to proliferation by transforming growth factor beta1. J. Biol. Chem. 274:12197–12200.
25. **Verschueren, K., J. E. Remacle, C. Collart, H. Kraft, B. S. Baker, P. Tylzanowski, L. Nelles, G. Wuytens, M. T. Su, R. Bodmer, J. C. Smith, and D. Huylebroeck.** 1999. SIP1, a novel zinc finger/homeodomain repressor, interacts with Smad proteins and binds to 5′-CACCT sequences in candidate target genes. J. Biol. Chem. 274:20489–20498.
26. **Vidal, A., and A. Koff.** 2000. Cell-cycle inhibitors: three families united by a common cause. Gene 247:1–15.
27. **Wang, H., T. Goode, P. Iakova, J. H. Albrecht, and N. A. Timchenko.** 2002. C/EBPalpha triggers proteasome-dependent degradation of cdk4 during growth arrest. EMBO J. 21:930–941.
28. **Yan, Y., J. Frisen, M. H. Lee, J. Massague, and M. Barbacid.** 1997. Ablation of the CDK inhibitor p57Kip2 results in increased apoptosis and delayed differentiation during mouse development. Genes Dev. 11:973–983.
29. **Yoshida, Y., S. Tanaka, H. Umemori, O. Minowa, M. Usui, N. Ikematsu, E. Hosoda, T. Imamura, J. Kuno, T. Yamashita, K. Miyazono, M. Noda, T. Noda, and T. Yamamoto.** 2000. Negative regulation of BMP/Smad signaling by Tob in osteoblasts. Cell 103:1085–1097.
30. **Zhang, P., N. J. Liegeois, C. Wong, M. Finegold, H. Hou, J. C. Thompson, A. Silverman, J. W. Harper, R. A. DePinho, and S. J. Elledge.** 1997. Altered cell differentiation and proliferation in mice lacking p57KIP2 indicates a role in Beckwith-Wiedemann syndrome. Nature 387:151–158.
31. **Zhang, Y. W., N. Yasui, K. Ito, G. Huang, M. Fujii, J. Hanai, H. Nogami, T. Ochi, K. Miyazono, and Y. Ito.** 2000. A RUNX2/PEBP2alphaA/CBFA1 mutation displaying impaired transactivation and Smad interaction in cleidocranial dysplasia. Proc. Natl. Acad. Sci. USA 97:10549–10554.
32. **Zhu, H., P. Kavsak, S. Abdollah, J. L. Wrana, and G. H. Thomsen.** 1999. A SMAD ubiquitin ligase targets the BMP pathway and affects embryonic pattern formation. Nature 400:687–693.
33. **Zimmermann, M.** 1983. Ethical guidelines for investigations of experimental pain in conscious animals. Pain 16:109–110.BM

JOURNAL OF BONE AND MINERAL RESEARCH
Volume 19, Number 9, 2004
Published online on June 2, 2004; doi: 10.1359/JBMR.040515

SRC-1 Is Necessary for Skeletal Responses to Sex Hormones in Both Males and Females

Takashi Yamada,[1,2] Hirotaka Kawano,[1,2] Keisuke Sekine,[2] Takahiro Matsumoto,[2,3] Toru Fukuda,[2] Yoshiaki Azuma,[4] Keiji Itaka,[1] Ung-il Chung,[5] Pierre Chambon,[6] Kozo Nakamura,[1] Shigeaki Kato,[2,3] and Hiroshi Kawaguchi[1]

ABSTRACT: We created *SRC-1*$^{-/-}$ mice by mating floxed SRC-1 mice with CMV-Cre transgenic mice. The *SRC-1*$^{-/-}$ mice showed high turnover osteopenia under physiological conditions and hardly responded to osteoanabolic actions of exogenous androgen and estrogen in males and females, respectively, after gonadectomies, indicating that SRC-1 is essential for the maintenance of bone mass by sex hormones.

Introduction: Steroid receptor coactivator-1 (SRC-1) is the first identified coactivator of nuclear receptors. This study investigated the role of SRC-1 in skeletal tissues of males and females using the deficient (*SRC-1*$^{-/-}$) mice.
Materials and Methods: *SRC-1*$^{-/-}$ mice were generated by mating our original floxed SRC-1 mice with CMV-Cre transgenic mice. Bone metabolism between 24-week-old *SRC-1*$^{-/-}$ and wildtype (WT) littermates under physiological conditions was compared in males and females by radiological, histological, and biochemical analyses. Difference of skeletal responses to steroid hormones was examined by gonadectomies and exogenous administration experiments with the hormones. Statistical analysis was performed by ANOVA determined by posthoc testing using Bonferroni's method.
Results and Conclusions: Although *SRC-1*$^{-/-}$ mice showed no abnormality in growth or major organs, both males and females showed osteopenia with high bone turnover in the trabecular bones, but not in the cortical bones, compared with WT littermates. Their serum levels of sex hormones were upregulated, suggesting a compensatory reaction for the insensitivity to these hormones. Gonadectomies caused decreases in BMDs of *SRC-1*$^{-/-}$ and WT mice to the same levels; however, replacement with 5α-dihydrotestosterone and 17β-estradiol in males and females, respectively, failed to restore the bone loss in *SRC-1*$^{-/-}$, whereas the WT bone volume was increased to the sham-operated levels. In contrast, bone loss by administered prednisolone was similarly seen in *SRC-1*$^{-/-}$ and WT mice. We conclude that SRC-1 is essential for the maintenance of bone mass by sex hormones, but not for the catabolic action of glucocorticoid, under both physiological and pathological conditions.
J Bone Miner Res 2004;19:1452—1461. Published online on June 2, 2004; doi: 10.1359/JBMR.040515

Key words: steroid hormone, coactivator, estrogen, androgen, glucocorticoid, bone

INTRODUCTION

STEROID HORMONES ARE involved in mediating important physiological processes in numerous target tissues including breast, uterus, brain, and bone. The actions are mediated by their binding to structurally homologous nuclear receptors, which act as ligand-dependent transcription factors to either activate or repress target gene expression.[1–3] Among steroid hormones, the sex steroids estrogens and androgens are essential for normal skeletal development and maintenance of healthy bone remodeling during life.[4–7] Estrogen deficiency causes osteoporosis with high bone turnover in postmenopausal women, and this disorder can be prevented or reversed by estrogen replacement. Androgens are also known to exert beneficial effects on the maintenance of normal bone mass and remodeling. Patients with hypogonadism or androgen receptor (AR) defect often develop osteoporosis with high bone turnover, and testosterone supplementation can restore the BMD in eugonadal osteoporotic men.[8] Contrary to the bone-sparing actions of estrogens and androgens, another steroid hormone, glucocorticoids, stimulate bone resorption and inhibit bone formation in humans and consequently lead to a decrease in bone mass. Excess glucocorticoids in vivo, as a result of either prolonged steroid therapy or Cushing's syndrome, lead to the development of osteoporosis, the degree of which seems to be related to the duration and dose of treatment.[9,10]

Expressions of nuclear receptors of these steroid hormones, estrogen receptors (ERs), ARs, and glucocorticoid

The authors have no conflict of interest.

[1]Department of Orthopaedic Surgery, Faculty of Medicine, University of Tokyo, Tokyo, Japan; [2]Institute of Molecular and Cellular Biosciences, University of Tokyo, Tokyo, Japan; [3]SORST, Japan Science and Technology, Saitama, Japan; [4]Pharmacological Research Department, Teijin Co. Ltd., Tokyo, Japan; [5]Department of Tissue Engineering, Faculty of Medicine, University of Tokyo, Tokyo, Japan; [6]Institut de Genetique et de Biologie Moleculaire et Cellulaire, Universite Louis Pasteur, College de France, Strasbourg, France.

receptor (GRs), in bone have been identified mainly in osteoblasts and bone marrow cells.[4,5] The transcriptional activities of the receptors are mediated by interaction with several classes of coactivators/corepressors in a ligand-dependent manner.[11,12] The first characterized steroid receptor coactivator (SRC) family contains three homologous members: SRC-1, SRC-2 (also known as TIF2 and GRIP1), and SRC-3 (also known as p/CIP, AIB1, RAC3, ACTR, and TRAM-1).[13–16] The SRC coactivators have been reported to function in several ways: recruitment of histone acetyltransferases, histone methyltransferases, interaction with other coactivators, and contact with certain general transcription factors.[13] There are several pieces of evidence that the SRC coactivators play important roles clinically in mediating the response to steroid hormones. A chromosomal translocation that involves SRC-2 was identified in acute myeloid leukemia.[17] SRC-3 overexpression was documented in breast, ovarian, and pancreatic cancer.[18,19] These data suggest the possibility that the SRC family could modulate the response to steroid hormones in bone as well.

SRC-1 was originally cloned as a strong transactivator of GR[14] and has been reported to enhance the actions of many nuclear receptors, including ERs and AR.[13] Clinical involvement of SRC-1 has not yet been found; however, its in vivo function has been investigated by analyses of the *SRC-1*–deficient mice created by the O'Malley group using a conventional gene targeting method.[20] There were no apparent abnormalities in their major organs except for a partial resistance to sex hormones and thyroid hormone.[20–23] Aiming at generating double/triple mutant mice with tissue-specific *SRC-1* deficiency and other cofactor gene mutations such as SRC-2 and SRC-3 without embryonic lethality in the future, we first created floxed *SRC-1* mice in which the SRC-1 gene locus was flanked by loxP sites. In this study, the first using the floxed mice, we generated *SRC-1*–deficient ($SRC\text{-}1^{-/-}$) mice, whose SRC-1 function was generally blocked, by mating them with CMV-Cre transgenic mice. To define the functions of SRC-1 in skeletal tissues of both males and females, we analyzed the bone phenotype of the $SRC\text{-}1^{-/-}$ mice under physiological conditions and under stimulation by estrogens, androgens, or glucocorticoids.

MATERIALS AND METHODS

Generation of SRC-$1^{-/-}$ *mice*

Mouse SRC-1 genomic clones were obtained by screening an embryonic stem (ES) cell genomic library in λ phage (Stratagene) using human SRC-1 cDNA as a probe. A 20-kb fragment of mouse SRC-1 containing exons 3–5, encoding the basic-helix-loop-helix (bHLH) domain, was used to construct the targeting vector (Fig. 1A). The targeting vector consisted of a 7.7-kb 5′ homologous region containing exon 4, a 3.3-kb 3′ homologous region, a single loxP site, and the phosphoglycerate kinase-neomycin (PGKneo) cassette between the two loxP sites. The linearized targeting vector was electroporated into ES cells (25 μg/1.0 × 10^7 cells) using a Gene Pulser II (Bio-Rad Laboratories) at 250 V and 500 μF, and G418 neomycin-resistant clones were expanded as described previously.[24] Two ES cell clones (Fig. 1B, 4p29 and 4q30) containing a targeted *SRC-1L3* allele were identified by Southern blot analysis of *Eco*RI-digested ES cell genomic DNA, using 5′ (probe 1) and 3′ (probe 2) external probes and a neomycin probe. Targeted ES cells were aggregated with single eight-cell embryos from ICR mice (CLEA Japan) and returned to a pseudopregnant host of the same strain to generate chimeras as described previously.[24] Chimeric males were crossed with C57BL/6J females (CLEA Japan) to produce germ line transmission of the targeted *L3* allele. $SRC\text{-}1^{L3/L3}$ mice were then crossed with the CMV-Cre transgenic mice to generate $SRC\text{-}1^{L-/+}$ (also designated as $SRC\text{-}1^{+/-}$) mice (mice bearing one allele in which exon 4 and the neomycin cassette were deleted). Inbreeding of $SRC\text{-}1^{L-/+}$ mice yielded $SRC\text{-}1^{L-/L-}$ (also designated as $SRC\text{-}1^{-/-}$) mice homozygous for the deletion of SRC-1 exon 4. Because $SRC\text{-}1^{L3/L3}$ mice and CMV-Cre transgenic mice were in different strains, all $SRC\text{-}1^{-/-}$ mice used in this study had been backcrossed for 10 generations into the C57BL/6 background.

Animal conditions

All mice were kept in plastic cages under standard laboratory conditions with a 12-h dark, 12-h light cycle and a constant temperature of 23°C and humidity of 48%. The mice were fed a standard rodent diet (CE-2; CLEA Japan) containing 25.2% protein, 4.6% fat, 4.4% fiber, 6.5% ash, 3.44 kcal/g, 2.5 IU vitamin D_3/g, 1.09% calcium, and 0.93% phosphorus with water ad libitum. In each experiment, homozygous wildtype (WT) and $SRC\text{-}1^{-/-}$ mice that were littermates generated from the intercross between heterozygous mice were compared. All experiments were performed according to the protocol approved by the Animal Care and Use Committee of the University of Tokyo.

RT-PCR analysis

Total RNA was extracted from excised femora and tibias using an ISOGEN kit (Wako Pure Chemical Industries) and reverse transcribed using XL reverse transcriptase (Takara Shuzo Co.) and an oligo (dT) primer (Takara Shuzo Co.). After first-strand cDNA synthesis, 5% of the reaction mixture was amplified with r-*Taq*DNA polymerase (Takara Shuzo Co.) using specific primer pairs: 5′-CATGTAGGCCATGAGG TCCACCAC-3′ and 5′-TGAAGGTCGGTGTGAACGGATTTGGC-3′ for G3PDH; 5′-TACTGAGAAGAGGCGCAGGG-3′ and 5′-CCAGAAGAAGAGGGCCCAGC-3′ for SRC-1 (exon 4-exon 5); and 5′-ATGAGTGGCCTTGGGGACAG-3′ and 5′-CCAGAAGAAGAGGGCCCAGC-3′ for SRC-1 (exon 3-exon 5). Up to 35 cycles of amplification were performed, with each cycle consisting of 96°C for 30 s, 55°C for 60 s, and 72°C for 60 s.

Western blot analysis

To detect SRC-1 protein expression, bone cell lysates were separated by SDS-PAGE and transferred onto nitrocellulose membranes. Membranes were probed with a goat polyclonal antibody raised against a carboxyl terminus peptide of human SRC-1 that is identical to the corresponding mouse sequence (1:1000 dilution, C-20; Santa Cruz Biotechnology) and a rabbit polyclonal antibody raised against a recombinant protein corresponding to amino acids 350–

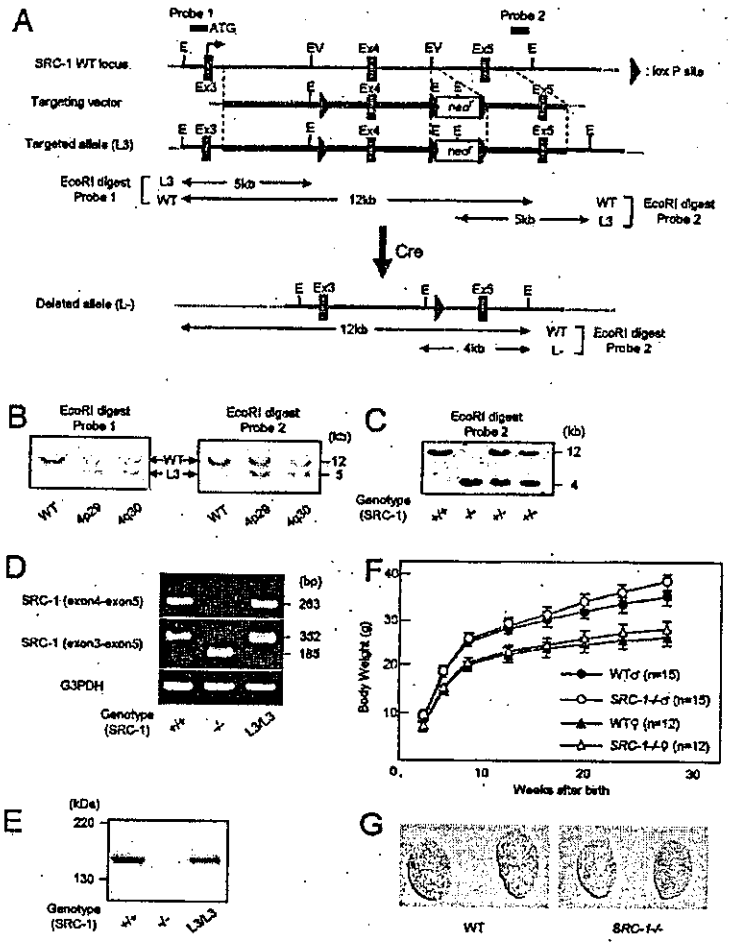

FIG. 1. Targeted disruption of mouse *SRC-1* gene. (A) Strategy to generate *SRC-1*$^{-/-}$ mice showing the WT SRC-1 locus, the targeting vector, the targeted allele (*L3*), and the deleted allele (*L−*) obtained after Cre-mediated excision. Exons (Ex) are shown as shaded boxes. The location of probes 1 and 2 are indicated. E, *Eco*RI; EV, *Eco*RV; neo^r, PGKneo cassette. LoxP sites are indicated as black arrowheads. (B) Southern blot analysis of targeted ES clones. Genomic DNA from WT ES cells and homologous targeted clones (4p29 and 4q30) were digested with *Eco*RI for hybridization with probe 1 (left) and 2 (right). (C) Southern blot analysis of offspring of heterozygous mates with probe 2. (D) Detection of the SRC-1 transcript by RT-PCR in long bones of WT, *SRC-1*$^{-/-}$, and floxed *SRC-1* (*SRC-1*$^{L3/L3}$) mice. (E) Western blot analysis of the SRC-1 protein using an antibody against a carboxyl terminus of the SRC-1 peptide in long bones of WT, *SRC-1*$^{-/-}$, and floxed *SRC-1* (*SRC-1*$^{L3/L3}$) mice. (F) Growth curves determined by the body weight of WT and *SRC-1*$^{-/-}$ mice in both sexes. Data are expressed as means (symbols) ± SE (error bars) for 15 mice/group for males and 12 mice/group for females. There were no significant differences between WT and *SRC-1*$^{-/-}$ mice in either sex ($p > 0.05$). (G) Smaller testes were observed in male *SRC-1*$^{-/-}$ mice.

690 mapping within an internal region of SRC-1 of mouse origin (1:1000 dilution, M-341; Santa Cruz Biotechnology) and then a peroxidase-conjugated second antibody. Blots were visualized using an ECL detection kit (Amersham Biosciences).

Radiological analysis

Bone radiographs of excised femora, tibias, and the fifth lumbar vertebrae from 12-, 16-, and 24-week-old WT and *SRC-1*$^{-/-}$ littermates were taken using a soft X-ray apparatus (model CMB-2; SOFTEX). BMD was measured by DXA using a bone mineral analyzer (PIXImus Mouse Densitometer; GE Medical Systems). CT was performed with a pQCT analyzer (XCT Research SA+; Stratec Medizintecnik) operating at a resolution of 80 μm. Metaphyseal pQCT scans of femora were performed to measure the trabecular volumetric BMD. The scan was positioned in the metaphysis at 1.2 mm proximal from the distal growth plate. This area contains cortical as well as trabecular bone. The trabecular bone region was defined by setting the threshold to 395 mg/cm^3 according to a previous report.[25] Mid-diaphyseal pQCT scans of femora were performed to determine the cortical volumetric BMD and the cortical thickness. The mid-diaphyseal region of femora in mice contains mostly cortical bone. The cortical bone region was defined by setting the threshold to 690 mg/cm^3.[25] The interassay CVs for the pQCT measurements were <2%. μCT scanning of the fifth lumbar vertebrae was performed using a composite X-ray analyzer (model NX-CP-C80H-IL; Nittetsu ELEX Co.), and a total of 300 cross-sectional tomograms per vertebra were obtained with a slice thickness of 10 μm and reconstructed at 12 × 12 pixels into a 3D feature by the volume-rending method (software, VIP-Station; Teijin System Technology) using a computer (model SUN SPARK-5; Sun Microsystems). Electronic sections were cut in the transverse, coronal, and sagittal planes on 3D reconstructed images.

Histological analysis

Histological analyses were performed using 24-week-old WT and *SRC-1*$^{-/-}$ littermates. For von Kossa and toluidine blue stainings, lumbar vertebrae were fixed with 70% ethanol, embedded in glycol methacrylate without decalcification, and sectioned in 3-μm slices using a microtome (model 2050; Reichert Jung). For calcein double labeling,

mice were injected subcutaneously with 16 mg/kg body weight of calcein at 10 and 3 days before death. Sections with toluidine blue stainings were used to visualize calcein labels under fluorescent light microscopy. $TRACP^+$ cells were stained at pH 5.0 in the presence of L(+)-tartaric acid using naphthol AS-MX phosphate (Sigma-Aldrich Co.) in *N,N*-dimethyl formamide as the substrate. The specimens were subjected to histomorphometric analyses using a semi-automated system (Osteoplan II; Carl Zeiss), and measurements were made at 400× magnification. Parameters for the trabecular bone were measured in an area 0.3 mm in length from the cortical bone at the fifth lumbar vertebrae. Nomenclature, symbols, and units are those recommended by the Nomenclature Committee of the American Society for Bone and Mineral Research.[26]

Serum and urinary biochemistry

Blood samples from 24-week-old WT and *SRC-1*$^{-/-}$ littermates (n = 15/genotype for males and n = 12/genotype for females) were collected by heart puncture under Nembutal (Dainippon Pharmaceutical Co.) anesthesia, and urine samples were collected for 24 h before death using oil-sealed bottles in metabolism cages (CL-0305; CLEA Japan). The levels of calcium, phosphorus, and alkaline phosphatase activity in serum were measured using a calcium HR kit (Wako Pure Chemical Industries), an inorganic phosphorus II kit (Wako Pure Chemical Industries), and a liquitech alkaline phosphatase kit (Roche Diagnostics), respectively, with an autoanalyzer (type 7170; Hitachi Hith-Technologies). Serum osteocalcin levels were measured using the competitive radioimmunoassay (RIA) kit (Biomedical Technologies). Serum testosterone and 17β-estradiol (E_2) levels were measured using RIA kits (Diagnostic Products), and serum leptin was assayed with the ELISA-based Quantikine M mouse leptin immunoassay kit (R&D Systems). Urinary deoxypyridinoline was measured using the Pyriliks-D ELISA (Metra Biosystems). The values were corrected according to urinary creatinine (Cr), as measured by a standard colorimetric technique with an autoanalyzer (type 7170).

Gonadectomy and hormone treatment

Male WT and *SRC-1*$^{-/-}$ littermates were orchidectomized or sham-operated at 16 weeks of age and implanted subcutaneously with 60-day time-release pellets (Innovative Research of America) containing either placebo or 5α-dihydrotestosterone (DHT; 10 mg/pellet; 8 mice/group). Female WT and *SRC-1*$^{-/-}$ littermates were ovariectomized or sham-operated at 16 weeks of age and implanted subcutaneously with 60-day time-release pellets containing either placebo or E_2 (0.025 mg/pellet; 8 mice/group). For the glucocorticoid experiment, male WT and *SRC-1*$^{-/-}$ littermates were implanted subcutaneously with 60-day time-release pellets containing either placebo or prednisolone (4 mg/pellet) at 16 weeks of age (8 mice/group). BMD of the fifth lumbar vertebrae was measured in situ by DXA using a bone mineral analyzer (PIXImus Mouse Densitometer) at 16 and 24 weeks. All mice were killed at 24 weeks of age, seminal vesicles of male and uteri of female mice were excised and weighed, and BMD of the excised fifth lumbar vertebrae was measured by DXA.

Statistical analysis

All data are expressed as means ± SE. Means of groups were compared by ANOVA, and significance of differences was determined by posthoc testing using Bonferroni's method.

RESULTS

Generation of SRC-1$^{-/-}$ *mice by a Cre-loxP system*

We targeted exon 4 of the *SRC-1* gene, which encodes the bHLH domain to generate functionally null SRC-1 mutant mice (Fig. 1A). The targeting vector was designed with three loxP sites flanking exon 4 and the PGKneo cassette. Complete excision of exon 4 and floxed PGKneo cassette in the *L3* allele mediated by Cre recombinase was confirmed in the genomic DNA sequence of F_2 offspring, and the mutation resulted in the creation of a stop codon at exon 5 by splicing exon 3 and 5 transcripts. Thus, the truncated protein produced from the deleted allele lacks the C-terminal region that includes all SRC-1 functional domains for transcriptional activation, histone acetyltransferase activity, and interactions with nuclear receptors, CBP, P300, and p/CAF.[14,27,28]

Chimeric males derived from targeted L3 ES clones transmitted the mutation through their germline, yielding floxed *SRC-1* (*SRC-1*$^{L3/L3}$) mice. Floxed *SRC-1* mice grew normally and exhibited no overt abnormalities with normal SRC-1 mRNA and protein expression levels (Figs. 1D and 1E). Floxed *SRC-1* mice were crossed with CMV-Cre transgenic mice to generate SRC-1 heterozygous (*SRC-1*$^{+/-}$) mice. Inbreeding of heterozygous *SRC-1*$^{+/-}$ mice yielded *SRC-1*$^{-/-}$ mice in accordance with Mendelian expectations (Fig. 1C). Short SRC-1 transcripts exclusive of exon 4 were detected by RT-PCR in the long bones of *SRC-1*$^{-/-}$ mice (Fig. 1D); however, because of the creation of a stop codon at exon 5, no SRC-1 protein expression was shown by Western blot analysis using an antibody against a carboxyl terminus of the SRC-1 peptide, confirming disruption of the *SRC-1* gene (Fig. 1E). Similar mRNA and protein expression patterns were observed in tissues including liver, kidney, isolated primary osteoblasts, and bone marrow cells, even when we used other primer sets and antibodies (data not shown).

Both male and female *SRC-1*$^{-/-}$ mice grew normally and were apparently indistinguishable from WT littermates. Growth curves determined by the body weight were somewhat similar between WT and *SRC-1*$^{-/-}$ mice in both males and females during the observation period up to 28 weeks, although a slight increase of body weight caused by obesity was seen in both sexes of *SRC-1*$^{-/-}$ mice as they got older (Fig. 1F). While no abnormality of reproductive organs, including ovary and uterus, was found in female *SRC-1*$^{-/-}$ mice, a slight hypoplasia of testis was seen (~20% in weight) in males (Fig. 1G). These abnormalities were the same as those reported in the *SRC-1*–deficient mice generated by a conventional method.[20]

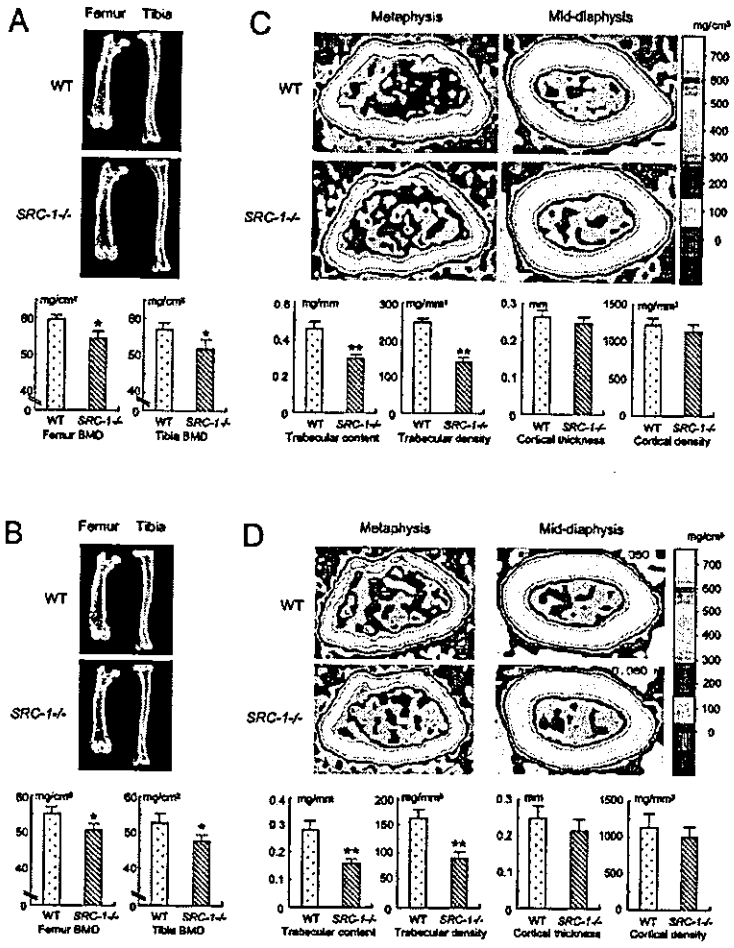

FIG. 2. Radiological findings of the long bones in *SRC-1*$^{-/-}$ and WT littermates. (A and B) Plain X-ray images of femur and tibia in representative (A) males and (B) females of both genotypes at 24 weeks of age. The BMD of the entire femurs and tibias measured by DXA is shown in the graphs below. (C and D) pQCT images of the distal metaphysis (left) and the mid-diaphysis (right) of the femurs in representative (C) males and (D) females of both genotypes at 24 weeks of age. The color gradient indicating BMD is shown in the right bars. The trabecular content and density at the metaphysis and the cortical thickness and density at the mid-diaphysis are shown in the graphs below. Data in all graphs are expressed as means (bars) ± SE (error bars) for 15 mice/group for males and 12 mice/group for females. Significant difference from WT: $*p < 0.05$, $**p < 0.01$.

Osteopenia in male and female SRC-1$^{-/-}$ *mice*

To learn the physiological role of SRC-1 in skeletal tissues, we analyzed the long bones and vertebrae of *SRC-1*$^{-/-}$ mice. The lengths of the long bones and the trunk of these mice were similar to those of WT littermates, at least during the observation period up to 24 weeks of age, indicating that SRC-1 is not involved in the regulation of skeletal growth. BMD was similar between long bones of the two genotypes at 12 weeks of age and tended to be lower in *SRC-1*$^{-/-}$ than WT mice at 16 weeks, although this was not statistically significant (data not shown). At 24 weeks, however, *SRC-1*$^{-/-}$ mice showed ~10% less BMD of long bones than WT littermates in males (Fig. 2A) and females (Fig. 2B). When trabecular and cortical bones were analyzed separately in the femora using pQCT, *SRC-1*$^{-/-}$ mice showed ~35–45% lower BMC and BMD of trabecular bones; however, the cortical bones were not affected by the SRC-1 deficiency in either males (Fig. 2C) or females (Fig. 2D).

To investigate the abnormalities of the *SRC-1*$^{-/-}$ trabecular bones in more detail, we performed morphological analyses of vertebral bodies that are rich in trabecular bone in males and females at 24 weeks of age. 3D CT analysis of the fifth lumbar vertebrae confirmed the decrease in *SRC-1*$^{-/-}$ trabecular bone in both sexes (Fig. 3).

Histomorphometric analyses confirmed that the bone volumes (BV/TV) were decreased by 30–40% in the *SRC-1*$^{-/-}$ males and females compared with those of WT littermates (Table 1). Parameters for both bone formation (Ob.S/BS, MAR, and BFR) and resorption (N.Oc/B.Pm, Oc.S/BS, and ES/BS) were also significantly higher in *SRC-1*$^{-/-}$ mice. The increase in bone resorption parameters (~60–80%) exceeded that in bone formation parameters (~30–60%), indicating a state of high-turnover osteopenia that is characteristic of osteoporosis with sex hormone deficiency.

Biochemical markers in the serum and urine supported the increase of bone turnover by SRC-1 deficiency (Table 2). Bone formation markers (serum alkaline phosphatase and osteocalcin) and a bone resorption marker (urinary deoxypyridinoline) were higher in both males and females of *SRC-1*$^{-/-}$ mice than those in WT littermates. The serum calcium and phosphorus levels were similar between the two genotypes, suggesting that the skeletal abnormalities by SRC-1 deficiency were not the result of the changed calcium or phosphorus levels. Considering that *SRC-1*$^{-/-}$ mice

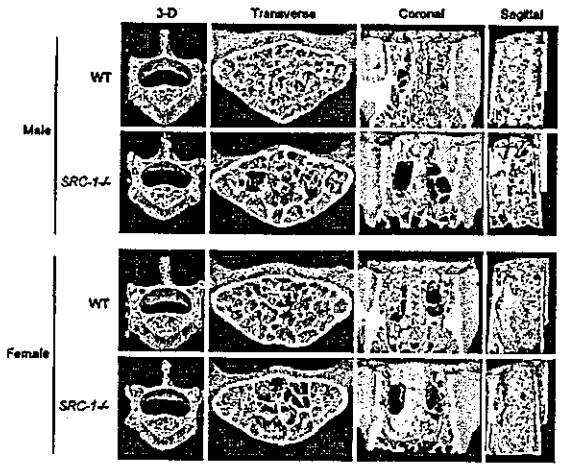

FIG. 3. Radiological and histological findings of the lumbar vertebrae in *SRC-1*$^{-/-}$ and WT littermates. 3D CT images of the fifth vertebrae in representative males and females of both genotypes at 24 weeks of age. The BMD of the entire fifth vertebrae measured by DXA was 58.7 ± 3.5 (male WT), 49.0 ± 2.1 (male *SRC-1*$^{-/-}$), 48.7 ± 3.3 (female WT), and 41.6 ± 1.4 mg/cm^2 (female *SRC-1*$^{-/-}$) for 15 mice/group for males and 12 mice/group for females. There were significant differences between WT and *SRC-1*$^{-/-}$ in both sexes ($p < 0.05$).

showed a slight obesity at this age, we measured the serum level of leptin, which has recently been reported to be an antiosteogenic factor. The level was somewhat upregulated, although not significantly, in *SRC-1*$^{-/-}$ mice. Interestingly, despite the high bone turnover, the serum levels of both testosterone in males and estradiol in females were elevated in *SRC-1*$^{-/-}$ mice, suggesting a compensatory mechanism in the endocrine system for the insensitivity to these sex hormones.

Insensitivity to administration of sex hormones in gonadectomized SRC-1$^{-/-}$ *mice*

To examine the involvement of SRC-1 in the skeletal actions of sex hormones, we performed hormone administration experiments (Figs. 4A–4D). After orchidectomy and ovariectomy on males and females, respectively, at 16 weeks of age, a slow-releasing pellet of sex hormone or placebo was subcutaneously implanted, and BMD was measured at 24 weeks. Effects of gonadectomies and hormone replacements were confirmed by seminal vesicle and uterine weights of males and females, respectively (Table 3). Both orchidectomy and ovariectomy markedly decreased these weights in WT and *SRC-1*$^{-/-}$ mice. DHT and E_2 restored them to the levels similar to those of sham-operated mice in WT, whereas these hormones restored almost one-half of them in *SRC-1*$^{-/-}$ mice, which is consistent with a previous study using another *SRC-1* knockout mouse.[20] Regarding BMD, besides the raw BMD values (Figs. 4A and 4C), the percent changes from baseline to final BMD during 8 weeks (Figs. 4B and 4D) were also compared between WT and *SRC-1*$^{-/-}$ mice. Both orchidectomy and ovariectomy decreased bone volumes of the two genotypes to the same levels in both sexes (~45.0 mg/cm^2 in males and 38.5 mg/cm^2 in females). When slow-releasing pellets of DHT and E_2 were subcutaneously implanted in the gonadectomized males and females, respectively, they prevented bone loss in WT mice. However, these hormone replacements restored little of the bone loss in *SRC-1*$^{-/-}$ mice, indicating that SRC-1 deficiency impairs the skeletal responses to sex hormones in both males and females.

We further examined the contribution of SRC-1 to the catabolic action of glucocorticoids on bone (Figs. 4E and 4F). When a slow-releasing pellet of prednisolone was implanted at 16 weeks, BMD was reduced similarly in WT and *SRC-1*$^{-/-}$ littermates, ~10% during the following 8 weeks, suggesting that SRC-1 is not essential in the bone catabolic action of glucocorticoids mediated by GR.

DISCUSSION

In this study, we originally generated *SRC-1*$^{-/-}$ mice by means of a Cre-loxP system and confirmed the lack of *SRC-1* gene expression in bone and other tissues. There is another *SRC-1* knockout mouse line that was generated by the O'Malley group, using a conventional gene targeting method.[20] Because both our *SRC-1*$^{-/-}$ mice and the conventional *SRC-1* knockout mice have similar genetic backgrounds by being extensively backcrossed into C57BL/6, we assume that the two mice should exhibit similar phenotypes. Modder et al.[29] recently reported skeletal phenotypes of the conventional *SRC-1* knockout mice showing resistance to the osteoanabolic action of estradiol in ovariectomized females, which is consistent with our results. Comparison of the two knockout mice is summarized in Table 4. In the conventional knockout mice, the targeting event inserted an in-frame stop codon at the Met (381) in exon 11, causing the downstream deletion of genomic sequence. Although the RNA encoding the bHLH-PAS domain was normally expressed in the knockout mice, all SRC-1 functional domains for transcriptional activation were confirmed to be disrupted, and it was not likely to have a dominant negative effect, because the bHLH-Per-Arnt-Sim (PAS) domain interacted with neither the full-length SRC-1 nor other SRC-1 family members such as TIF2.[20] In our *SRC-1*$^{-/-}$ mice, a stop codon created in the middle of the bHLH-PAS domain at exon 5 predicts a truncated product that is shorter than that in the conventional *SRC-1* knockout mice. Besides the skeletal finding in female mice in the previous report,[29] this study revealed that the SRC-1 deficiency also caused resistance to osteoanabolic action of androgen in orchidectomized males and no abnormality in osteocatabolic action of glucocorticoids. Discrepancy between the previous and present studies seems to be the bone phenotype under physiological conditions: their conventional *SRC-1* knockout mice did not exhibit osteopenia, whereas our *SRC-1*$^{-/-}$ mice did. We believe, however, that this discrepancy is caused by the difference in age when the analyses were done: 12 weeks for them versus 24 weeks for us. In fact, our study also did not detect significant difference of BMD at 12 weeks between WT and *SRC-1*$^{-/-}$ littermates of either sex under physiological conditions. It is speculated that, with aging, the compensatory elevation of